

CERTIFICATION OF APPROVAL

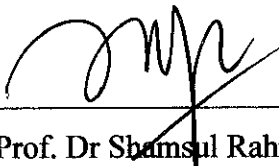
Adsorption of Copper, Zinc and Iron using Microwave Incinerated Rice Husk Ash (MIRHA) Columns

by

Faiz Hafzan bin Fauzi

A project dissertation submitted to the
Civil Engineering Programme
Universiti Teknologi PETRONAS
in partial fulfilment of the requirement for the
BACHELOR OF ENGINEERING (Hons)
(CIVIL ENGINEERING)

Approved by.



(Assoc. Prof. Dr Shamsul Rahman Mohamed Kutty)

Universiti Teknologi PETRONAS
Tronoh, Perak

January 2008

**Adsorption of Copper, Zinc and Iron Using
Microwave Incinerated Rice Husk Ash (MIRHA)
Columns**

by

Faiz Hafzan bin Fauzi

A project dissertation submitted to the
Civil Engineering Programme
Universiti Teknologi PETRONAS for the
Bachelor of Engineering (Hons)
(Civil Engineering)

JAN 2008

Universiti Teknologi PETRONAS
Bandar Seri Iskandar
31750 Tronoh
Perak Darul Ridzuan

CERTIFICATION OF ORIGINALITY

This is to certify that I am responsible for the work submitted in this project, that the original work is my own except as specified in the references and acknowledgements, and that the original work contained herein have not been undertaken or done by unspecified sources or persons.



(FAIZ HAFZAN BIN FAUZI)

ABSTRACT

Microwave Incinerated Rice Husk Ash (MIRHA), produced from the rice husk is one of the low-cost materials that were used as a sorbent of heavy metal. It was proven by lots of researchers around the world about the potential of the rice husk ash with different method of preparation. The main objective of the project is to determine the adsorption rate of the MIRHA by using the column method. The effects of important factors, such as the flow rate, the influent concentration and bed depth will be studied.

The rice husk ash was burned in controlled temperature. Furthermore, to ensure the MIRHA is in the adsorption zone, the MIRHA need to be immersed in weak acid for 24 hours. The project continues by preparing the fixed-bed column with the MIRHA placed inside the column with three different bed heights. The project also varied by using the Zinc, Copper and Iron in aqueous solution as the influent. Thomas, Adams-Bohart, and Yoon-Nelson models were applied to experimental data to predict the breakthrough curves using non-linear regression and to determine the characteristic parameters of the column useful for process design.

The result obtained shows that MIRHA was capable of adsorbing 100 % of heavy metal with different rates. The types of influent and the bed height also influencing the breakthrough time. Thomas model was found suitable for the normal description of breakthrough curve at the experimental condition, while Adams-Bohart model was only for an initial part of dynamic behaviour of the rice husk column.

As the conclusion, the MIRHA is an efficient adsorbent and has a capable of removing 100 % the heavy metal in the experiment. The usage of MIRHA as the heavy metal removal can be commercialized and this method can be applied in the wastewater treatment plant. The initial region of breakthrough curve was defined by Adams-Bohart model at all experimental condition studied while the full description of breakthrough could be accomplished by Thomas models. Lastly, the objective of the project was achieved.

TABLE OF CONTENTS

ABSTRACT	iv
TABLE OF CONTENT	v
LIST OF FIGURES	vii
LIST OF TABLES	ix
CHAPTER 1: INTRODUCTION	1
1.1 Background Studies.....	1
1.2 Problem Statement.....	1
1.3 Objectives.....	2
1.4 Scope of Studies.....	2
CHAPTER 2: LITERATURE REVIEW	3
2.1 Impact of heavy metal.....	3
2.2 Adsorption.....	4
2.2.1 Column Adsorption.....	4
2.3 Breakthrough Curve.....	6
2.4 Rice Husk as the adsorbent.....	8
2.5 Fixed-bed isotherm Modelling.....	10
2.5.1 Thomas model.....	10
2.5.2 Adams-Bohart model.....	11
2.5.3 Yoon-Nelson model.....	11
CHAPTER 3: METHODOLOGY / PROJECT WORK	12
3.1 Burning of Rice Husk.....	12
3.2 Preparation of the MIRHA.....	12
3.3 Preparation of the stock solution of heavy metal.....	12
3.4 Apparatus setup.....	13
3.5 Calibration of flow rate.....	14
3.6 Measurement of heavy metal.....	14
3.7 Hazard Analysis.....	14

CHAPTER 4: RESULT AND DISCUSSION	15
4.1 Calibration of flow rate.....	15
4.2 Adsorption curve.....	16
4.2.1 Breakthrough curve for adsorption of Zinc.....	16
4.2.2 Breakthrough curve for adsorption of Copper.....	17
4.2.3 Breakthrough curve for adsorption of Iron.....	18
4.2.4 Breakthrough curve for adsorption of different influent.....	20
4.3 Modeling of breakthrough curve.....	22
4.3.1 Thomas model.....	22
4.3.2 Adams-Bohart model.....	29
4.3.3 Yoon-Nelson model.....	36
CHAPTER 5: CONCLUSION AND RECOMMENDATION	43
REFERENCE	44
APPENDICS	47

LIST OF FIGURES

Figure 2.1	: Definition of the breakthrough curve.....	5
Figure 2.2 (a)	: Breakthrough curve for different flowrate.....	7
Figure 2.2 (b)	: Breakthrough curve for different bed height.....	7
Figure 3.1	: The apparatus of the experiment.....	13
Figure 4.1	: Graph Flow rate vs. Pump Speed.....	15
Figure 4.2(a)	: Breakthrough curve for Zinc at different bed height ($C_o = 9.4\text{mg/L}$).....	16
Figure 4.2(b)	: Breakthrough curve for Copper at different bed height ($C_o = 16.1\text{ mg/L}$).....	17
Figure 4.2(c)	: Breakthrough curve for Iron at different bed height ($C_o = 9.9\text{ mg/L}$).....	18
Figure 4.3(a)	: Breakthrough curve of heavy metal at bed height 5 cm.....	20
Figure 4.3(b)	: Breakthrough curve of heavy metal at bed height 10 cm.....	21
Figure 4.3(c)	: Breakthrough curve of heavy metal at bed height 15 cm.....	21
Figure 4.4(a)	: Breakthrough curve obtained according to the Thomas Model (Zinc, $z=5\text{cm}$, $C_o = 9.4$).....	23
Figure 4.4(b)	: Breakthrough curve obtained according to the Thomas Model (Zinc, $z=10\text{cm}$, $C_o = 9.0$).....	23
Figure 4.4(c)	: Breakthrough curve obtained according to the Thomas Model (Zinc, $z=15\text{cm}$, $C_o = 9.0$).....	24
Figure 4.4(d)	: Breakthrough curve obtained according to the Thomas Model (Copper, $z=5\text{cm}$, $C_o = 16.1$).....	24
Figure 4.4(e)	: Breakthrough curve obtained according to the Thomas Model (Copper, $z=10\text{cm}$, $C_o = 16.1$).....	25
Figure 4.4(f)	: Breakthrough curve obtained according to the Thomas Model (Copper, $z=15\text{cm}$, $C_o = 16.1$).....	25
Figure 4.4(g)	: Breakthrough curve obtained according to the Thomas Model (Iron, $z=5\text{cm}$, $C_o = 9.9$).....	26
Figure 4.4(h)	: Breakthrough curve obtained according to the Thomas Model (Iron, $z=10\text{cm}$, $C_o = 9.9$).....	26
Figure 4.4(i)	: Breakthrough curve obtained according to the Thomas Model (Iron, $z=15\text{cm}$, $C_o = 9.9$).....	27
Figure 4.5(a)	: Relationship between Thomas rate constant (k_{Th}) with bed height.....	27
Figure 4.5(b)	: Relationship between maximum solid-phase concentrations (q_0) with bed height.....	28

Figure 4.6(a) : Breakthrough curve obtained according to the Adams-Bohart Model (Zinc, $z=5\text{cm}$, $Co = 9.4$).....	30
Figure 4.6(b) : Breakthrough curve obtained according to the Adams-Bohart Model (Zinc, $z=10\text{cm}$, $Co = 9.0$).....	30
Figure 4.6(c) : Breakthrough curve obtained according to the Adams-Bohart Model (Zinc, $z=15\text{cm}$, $Co = 9.0$).....	31
Figure 4.6(d) : Breakthrough curve obtained according to the Adams-Bohart Model (Copper, $z=5\text{cm}$, $Co = 16.1$).....	31
Figure 4.6(e) : Breakthrough curve obtained according to the Adams-Bohart Model (Copper, $z=10\text{cm}$, $Co = 16.1$).....	32
Figure 4.6(f) : Breakthrough curve obtained according to the Adams-Bohart Model (Copper, $z=15\text{cm}$, $Co = 16.1$).....	32
Figure 4.6(g) : Breakthrough curve obtained according to the Adams-Bohart Model (Iron, $z=5\text{cm}$, $Co = 9.9$).....	33
Figure 4.6(h) : Breakthrough curve obtained according to the Adams-Bohart Model (Iron, $z=10\text{cm}$, $Co = 9.9$).....	33
Figure 4.6(i) : Breakthrough curve obtained according to the Adams-Bohart Model (Iron, $z=15\text{cm}$, $Co = 9.9$).....	34
Figure 4.7(a) : Relationship between kinetic constant (k_{AB}) with bed height.....	34
Figure 4.7(b) : Relationship between maximum adsorption capacities (N_0) with bed height.....	35
Figure 4.8(a) : Breakthrough curve obtained according to the Yoon-Nelson Model (Zinc, $z=5\text{cm}$, $Co = 9.4$).....	36
Figure 4.8(b) : Breakthrough curve obtained according to the Yoon-Nelson Model (Zinc, $z=10\text{cm}$, $Co = 9.0$).....	37
Figure 4.8(c) : Breakthrough curve obtained according to the Yoon-Nelson Model (Zinc, $z=15\text{cm}$, $Co = 9.0$).....	37
Figure 4.8(d) : Breakthrough curve obtained according to the Yoon-Nelson Model (Copper, $z=5\text{cm}$, $Co = 16.1$).....	38
Figure 4.8(e) : Breakthrough curve obtained according to the Yoon-Nelson Model (Copper, $z=10\text{cm}$, $Co = 16.1$).....	38
Figure 4.8(f) : Breakthrough curve obtained according to the Yoon-Nelson Model (Copper, $z=15\text{cm}$, $Co = 16.1$).....	39
Figure 4.8(g) : Breakthrough curve obtained according to the Yoon-Nelson Model (Iron, $z=5\text{cm}$, $Co = 9.9$).....	39
Figure 4.8(h) : Breakthrough curve obtained according to the Yoon-Nelson Model (Iron, $z=10\text{cm}$, $Co = 9.9$).....	40
Figure 4.8(i) : Breakthrough curve obtained according to the Yoon-Nelson Model (Iron, $z=15\text{cm}$, $Co = 9.9$).....	40
Figure 4.9(a) : Relationship between the rate constant (k_{YN}) with bed height.....	41
Figure 4.9(b) : Relationship between the times required for 50% breakthrough (τ) with bed height.....	41

LIST OF TABLES

Table 2.1	: Reported maximum heavy metals adsorption capabilities (mg/g) for rice husk.....	9
Table 3.1	: The different bed depth of the column.....	13
Table 3.2	: Specific method for HACH® Spectrophotometer DR2800.....	14
Table 4.1	: Thomas model parameters at different condition using non-linear regression analysis.....	28
Table 4.2	: Adams–Bohart parameters at different conditions using non-linear regression analysis (up 50%).....	35
Table 4.3	: Yoon–Nelson parameters at different conditions using non-linear regression analysis.....	42

CHAPTER 1 : INTRODUCTION

1.1 Background Studies

Rice husk is a by product from rice milling. During the milling of paddy, about 78% of weight is received as rice, broken rice and bran while the other 22% of the weight of paddy is received as husk. The husk contains about 75% organic volatile matter and the balance 25% of the weight of the husk is converted into ash during the firing process, known as rice husk ash (RHA) (Feng et al., 2004). This RHA in turn contains around 85% - 90% of amorphous silica. In this project, the rice husk was burned in controlled temperature, which is about 500 °C in an incinerator, becomes the Microwave Incinerated Rice Husk Ash (MIRHA). (Elliot et al., 1981)

The ash produced after the husk has been burned, (RHA), is high in silica. A number of possible uses are being investigated. Rice husk contains lots of fiber, protein and some functional groups such as hydroxyl and amidogen, which make the adsorption process possible (Han et al, 2004). Furthermore, the yield of rice husk obtained from agriculture as a byproduct is vast. Hence rice husk is low cost and can be easily obtained.

1.2 Problem Statement

Different kinds of heavy metals exist in the solution with different forms, so their treatment methods are also different. In the adsorption method, rice husk ash has been used as one of the metal adsorbent. Since there are various types of heavy metals, the determination of the adsorption rate need to be further detailed.

1.3 Objective

The objective of the project is to use the adsorption column with the MIRHA as the adsorption medium inside the column and to determine the effectiveness of the MIRHA's adsorption from aqueous solution such as Copper (Cu^{2+}), Zinc (Zn^{2+}) and Iron (Fe^{2+}). In this method, the efficiencies of the MIRHA was also examined by varying the bed height.

1.4 Scope of Study

In the research, soluble heavy metal will be used as the specific heavy instead of using the raw wastewater in determining the adsorption process. The purpose is to examine the effect of the adsorption process by using different types of heavy metal at different time. The procedure and result of analysis from this study will be repeated by applying other heavy metal for further research.

CHAPTER 2 : LITERATURE REVIEW

The industries such as mining, metallurgy, machine manufacturing, chemical industry, electronics and instrument produce large quantities of heavy metal in wastewater every year, part of which is entered into water bodies without treatment, which results in the pollution of the aquatic environment. Heavy metals are cannot be degraded and ruined the natural conditions. They are usually ingested by aquatic animals and plants, as well as the crops on the land, and then enter into human body through food chain after high enrichment in the propagation's bodies. They accumulate in some organs of human body and cause chronic intoxication, which seriously endangers the health of human body (Lester et al., 1987). Therefore, heavy metal wastewater is a kind of industrial wastewater which seriously pollutes the environment and endangers human being.

Excessive release of toxic metals into the environment due to industrialization has created a great global concern. Monitoring and subsequent removal of toxic metals from the industrial effluents has, therefore, been made mandatory before their discharge into the environment. Copper (Cu^{2+}), Zinc (Zn^{2+}) and Iron (Fe^{2+}) ions in aqueous solutions are toxic (S.P. Mishra, 1997).

2.1 Impact of Heavy Metals

At least 20 metals are classified as toxic and half of these are emitted into the environment in quantities that pose risks to human health (Kortenkamp, 1996). Nickel is a common environmental pollutant and is toxic (e.g. in concentrations more than 15 mg/l), especially to activated sludge bacteria, and its presence is harmful to the operation of anaerobic digesters used in wastewater treatment plants (J.W. Patterson, 1977)

2.2 Adsorption

Adsorption generally can be defined as adhesion to the surface of solids with which they are in contact (Weber, 1972). Adsorption may occur through physical, chemical or ion-exchange processes (Weber, 1972). Physical adsorption on the external surface of a particle is based on Van der Waals forces of attraction. Chemical adsorption is characterized by the formation of chemical associations or bonds between ions or molecules from solution and the surfaces of particles which is mainly covalent (Weber, 1972; Reynolds, 1995). Adsorption which is based on ion exchanged is a chemical process whereby a negative or positive charge on a particle surface is equalized by ions possessing opposite charges. Adsorption is affected by pH, Eh, ionic strength, and the composition of the solution phase (Lester, 1987).

2.2.1 Column Adsorption

Design of a column for adsorption starts with laboratory testing to establish the breakthrough curve. At time intervals, the effluent from a column is sampled. Time zero is when the solution is applied to the column.

At first, the raw adsorbent is fresh with all its adsorption sites. Essentially none of the material to be removed escapes from the column. As time passes, some of the adsorption sites are used up, and concentration in the effluent rises (Han et al., 2006).

The shape of the graph may vary considerably for different situations. Usually there is a long time before the effluent concentration rises sharply and then levels off. If all the sites were occupied, we would expect the inlet concentration and the outlet concentrations to become the same (Han et al., 2006).

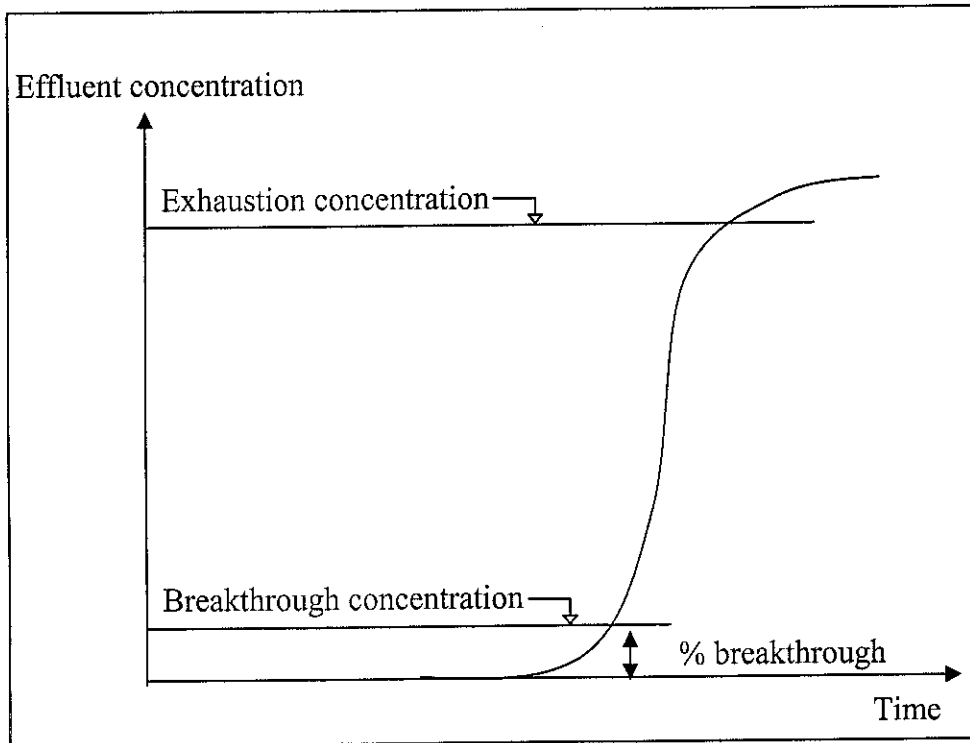


Figure 2.1 : Definition of the Breakthrough Curve

**Source : Aksu and Gonen, Prediction of breakthrough curves*

The breakthrough concentration is determined by the process specifications. This is the allowable concentration. If a pollutant is being removed, the breakthrough concentration might be the government regulation for what the effluent is discharged. For a commercial product where the column is removing color, the breakthrough concentration is determined by the specification for product quality. The point is that breakthrough concentration is not some fundamental number but depends on the decision to operate the process (McKay et al., 1999). The exhaustion concentration also depends on process considerations. When the benefits are not worth the costs, the column is considered exhausted.

2.3 Breakthrough Curve

Breakthrough curve is plot of relative concentration of a given substance versus time where relative concentration is defined as the ratio of the actual concentration. Breakthrough curve in Figure 2.2(a) shows the connection between the flow rate of the influent and time when determining the adsorption process using the column method. Studies confirmed that the breakthrough curves were dependent on flow rate, initial influent concentration and bed depth (Lester, 1987). The determination of adsorption efficiency also can be obtained from the breakthrough curve.

Figure 2.2(b) showed that adsorption model is very sensitive to a few parameters. The bed length, bed void fraction, flowrate and pellet diameter are four of the more sensitive parameters. Bed length and flowrate are fixed by design, so it is recommended that the bed void fraction be measured more accurately and minimized to increase the breakthrough time of the column. A more accurate estimate of the bed void fraction would greatly enhance the accuracy of the model. The pellet diameter also suggested to be minimized as much as allowable, avoiding a large pressure drop across the purifier (Aksu and Gonen, 2004).

A continuous fixed bed study was carried out by using rice husk as a biosorbent for the removal of Cu(II) from aqueous solution. The effects of important factors, such as the value of initial pH, the flow rate, the influent concentration of Cu and bed depth, were studied. The research studied and experimented confirmed that the breakthrough curves were dependent on flow rate, initial concentration and bed depth (Han et al., 2004).

From the study conducted there are variation of parameters that effects the efficiencies of the column adsorption such as bed height, flow rate, bed void fraction, adsorption particle diameter, ambient temperature and adsorption isotherm.

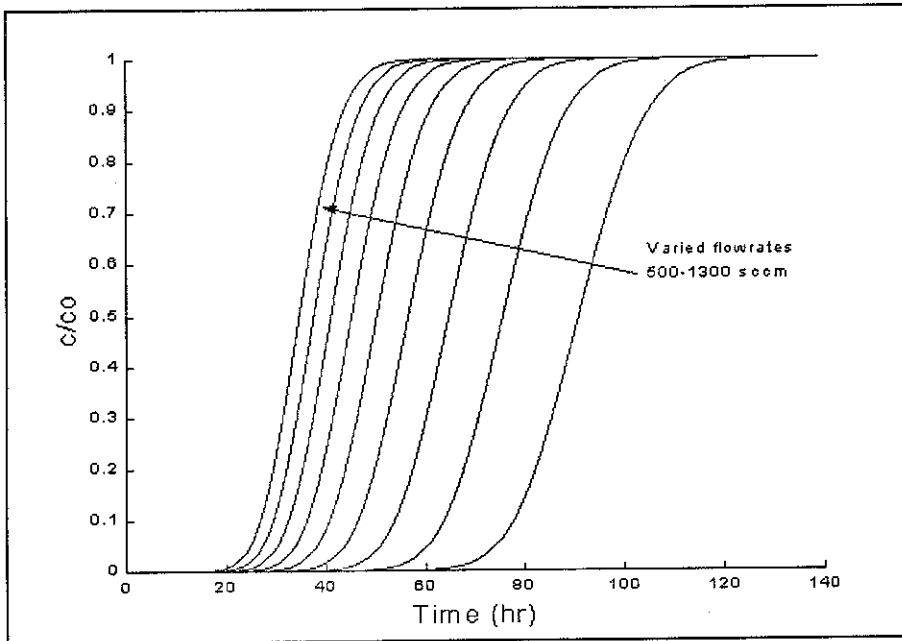


Figure 2.2 (a) : Breakthrough curve for different flowrate

*Source : Dicken et al / Gas Adsorption Group (2002)

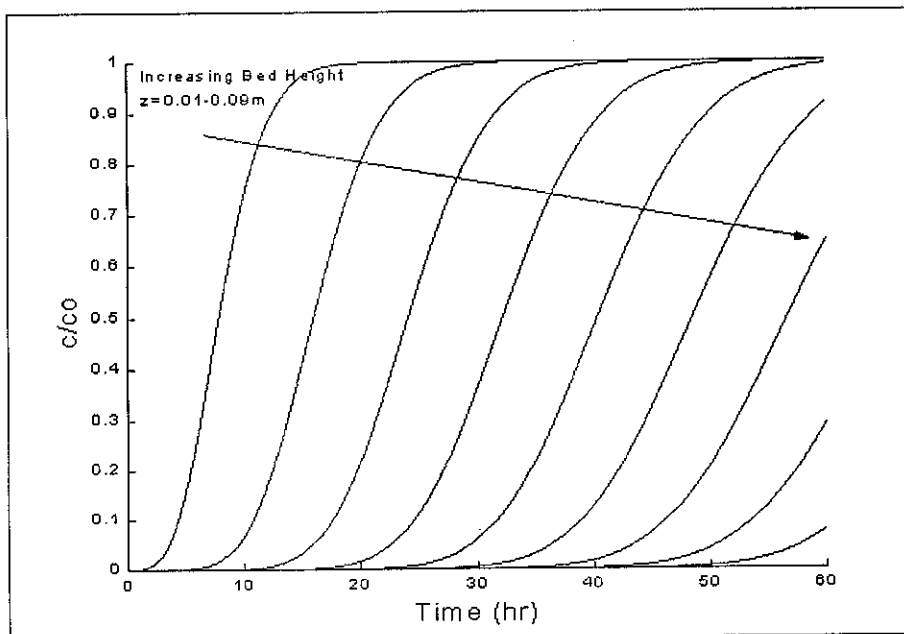


Figure 2.2 (b) : Breakthrough curve for different bed height

*Source : Dicken et al / Gas Adsorption Group (2002)

2.4 Rice Husk as the Adsorbent

Various methods used for the removal of metals from wastewaters include chemical precipitation, membrane filtration, ion exchange and adsorption. Adsorption using rice husk ash (RHA) as an adsorbent has now been studied and become one of the options in wastewater treatment.

Rice husk is an agricultural waste, obtained from the rice mills. It accounts for about one-fifth of the annual gross rice production of 545 million metric tons, of the world (Feng, 2004). Since RHA is available in plenty and it has very high potential as an adsorbent, recent study shows in detail the mesoporous characteristics of RHA and its adsorption characteristics for Copper, Zinc and Iron ions from aqueous solutions (Rahman, 2001).

Referring to the Table 2.1, shows the reported maximum heavy metals adsorption capabilities by the rice husk. It shows that the researchers has proved that different types of heavy metal has different impact in the adsorption capabilities of the rice husk. Although it refers to the other method of the adsorption process, it can be used as a references tu determine the adsorption capabilities of Zinc, Copper and Iron.

Table 2.1: Reported maximum heavy metals adsorption capabilities (mg/g) for rice husk

*Source : TG. Chuah et al / Desalination 175 (2005) 305-316

Heavy Metal	Researchers [ref]	Capabilities (mg/g)
As (V)	Roy et al., 1993 [55]	615.11
	Lee et al., 1999 [1]	18.98
	Nakbanpote et al., 2000 [2]	21.12
	Nakbanpote et al., 2002 [3]	39.84 (20°C) 50.50 (30°C) 64.10 (40°C)
Cd (II)	Roy et al., 1993 [55]	21.36
	Munaf and Zein, 1997 [56]	0.16
	Tarley et al., 2004 [10]	7 (modified with NaOH) 4 (unmodified with NaOH)
Co (II)	Marshall et al., 1993 [35]	0.32
Cr (III)	Marshall et al., 1993 [35]	1.9
Cr (VI)	Roy et al., 1993 [55]	164.31
	Munaf and Zein, 1997 [56]	4.02
	Guo et al., 2004 [2]	14.2-31.5
Cu (II)	Marshall et al., 1993 [35]	1.21
	Munaf and Zein, 1997 [56]	0.2
	Wong et al., 2003 [5]	29 (27°C) 22 (50°C) 18 (70°C)
	Wong et al., 2006 [6]	31.85 (single metal solution) 15.58 (bi-metal solution)
Hg	Tiwari et al., 1995 [57]	66.66 ($d_p = 37-50\mu\text{m}$) 55.55 ($d_p = 63-130\mu\text{m}$) 40.0 ($d_p = 130-600\mu\text{m}$)
Ni (II)	Marshall et al., 1993 [35]	0.23
Pb	Roy et al., 1993 [55]	11.4
	Wong et al., 2003 [5]	105 (27°C) 105 (50°C) 96 (70°C)
	Wong et al., 2003 [6]	129.48 (single metal solution) 48.31 (bi-metal solution)
	Tarley et al., 2004 [10]	21.55 (modified with NaOH) 45 (unmodified)
Zn	Marshall et al., 1993 [35]	0.75
	Mishra et al., 1997 [58]	26.94 (20°C) 28.25 (30°C) 29.69 (40°C) 30.80 (50°C)
	Munaf and Zein, 1997 [56]	0.173

2.5 Fixed-Bed Isotherm Modeling

The main purpose of the modeling is to determine and predict the performance of the heavy metal adsorption by the MIRHA. Thomas model, Adams-Bohart model and Yoon-Nelson model were used in this research.

2.5.1 Thomas model

The expression of Thomas model for an adsorption column is given as follows [(Aksu and Gonen, 2004), (Han et al., 2006) and (Thomas, 1994)]

$$\frac{C_t}{C_o} = \frac{1}{1 + \exp(K_{TH} q_o \frac{x}{v} - K_{TH} C_o t)} \quad (1)$$

where k_{Th} is the Thomas rate constant ($\text{ml min}^{-1} \text{mg}^{-1}$); q_o is the equilibrium heavy metal uptake per g of the adsorbent (mg/g); x is the amount of adsorbent in the column (g); C_o is the influent heavy metal concentration (mg/L); c_t is the effluent concentration at time t (mg/L); v is flow rate (mL/ min). The value of C_t/C_o is the ratio of effluent and influent CR concentrations.

The kinetic coefficient k_{Th} and the adsorption capacity of the column q_o can be determined from a plot of C_t/C_o against t at a given flow rate using the non-linear regression method.

2.5.2 The Adams-Bohart model

The Adams–Bohart model is used for the description of the initial part of the breakthrough curve. The expression is the following (Aksu and Gonen, 2004):

$$\frac{C_t}{C_o} = \exp(K_{AB}C_o t - k_{AB}N_o \frac{Z}{F}) \quad (2)$$

where k_{AB} is the kinetic constant ($l \text{ mg}^{-1} \text{ min}^{-1}$), F is the linear velocity calculated by dividing the flow rate by the column section area (cm min^{-1}), Z is the bed depth of column and N_o is the saturation concentration (mg/L).

From this equation, values describing the characteristic operational parameters of the column can be determined from a plot of C_t/C_o against t at a given bed height and flow rate using the non-linear regressive method.

2.5.3 The Yoon-Nelson model

The Yoon–Nelson equation regarding a single component system is expressed as (Aksu and Gonen, 2004):

$$\frac{C_t}{C_o - C_t} = \exp(K_{YN}t - \tau K_{YN}) \quad (3)$$

where k_{YN} is the rate constant (min^{-1}) and is τ , the time required for 50% adsorbate breakthrough (min).

The approach involves a plot of $C_t/(C_o - C_t)$ versus sampling time (t). The parameters of k_{YN} and τk_{YN} can be obtained using the non-linear regressive method.

CHAPTER 3 : METHODOLOGY/PROJECT WORK

3.1 Burning the Rice Husk Ash

The first procedure to be conducted is to burn the rice husk in the incinerator. The rice husk are burned at controlled temperature, 500° C, to increase the reactivity of the rice husk in adsorption process.

3.2 Preparation of the Microwave Incinerated Rice Husk Ash (MIRHA)

After the burning process, the MIRHA were immersed in the weak acid (pH 4.24, 0.5% concentration) for 24 hours. The purpose of this procedure is to adjust the pH of the rice husk ash into the acidic state to allow the adsorption process to occur. The pH of the solution affects the surface charge of the adsorbents as well as the degree of ionization and speciation of different pollutants (Elliott, 1981). Change in pH affects the adsorptive process through dissociation of functional groups on the active sites on the surface of the adsorbent and subsequently leads to a shift in reaction kinetics and the equilibrium characteristics of the adsorption process.

3.3 Preparation of the Stock Solution of the Heavy Metals

The preparation of the stock solution is done by using the heavy metal salt from the laboratory. The stock solution was prepared for 40 Litre with initial concentration of 10 ppm.

According to the calculation, 833.6 mg of Zinc Chloride soluble has been measured to prepare the Zinc solution, 1520.8 mg of Copper Chloride soluble for Copper solution and 1991.2 mg of Ferum (II) Sulphate soluble for Iron solution. The heavy metal salt was diluted using de-ionized water. To ensure the stock solution is 10 ppm, few samples from the solution were taken and measured using the spectrophotometer.

3.4 Apparatus Setup

Silicone tube were used as the column in the research. The column were placed at a holder that is suitable with the size and the diameter of the column (Figure 3.1). Glass beaker were placed at the bottom of the column for sampling process of the effluent.



Figure 3.1 : The apparatus of the experiment

In the experiment, three different bed depth of MIRHA was prepared to check the effect of the depth of the adsorption medium on the breakthrough of the heavy metal. The different bed depth also was to determine the optimum bed depth of the MIRHA as a result of the efficiency of heavy metal removal.

Table 3.1 : The bed different bed depth of the column

Column	Bed Depth (cm)
1	5
2	10
3	15

3.5 Calibration of flowrate

The calibration process is to determine the total effluent per day and setup the pump speed. The optimum flowrate for each adsorption column were examined using distilled water as the influent. The influent were maintained to be constant up to 1 cm above the bed as the distributed flow of distilled water in the bed assured.

3.6 Measurement of Heavy Metal

The concentration of influent and effluent of Copper, Zinc and Iron in the experiment were measured using spectrophotometer DR2800. The measurement of heavy metal using spectrophotometer needs a specific reagent to react with the solution.

Table 3.2 : Specific method for HACH® Spectrophotometer DR2800

Heavy Metal	Method	Range (mg/L)	Reagent
Copper	Bicinchoninate, Method 8026	0.04 to 5.00	Copper Reagent, CuVer® 2
Zinc	Zincon Method 8009	0.01 to 3.00	Zinc Reagent, ZincoVer® 5
Iron	FerroVer Method 8008	0.02 to 3.00	Iron Ferrous Reagent

3.7 Hazard Analysis

The project conducted must comply with Universiti Teknologi PETRONAS Health, Safety and Environment (HSE) rules and regulation. The HSE rules and regulation are meant to prevent accident or injuries, to avoid any harm to students and people surrounding, to prevent properties damage and loss event, and to take care of university image and performance.

CHAPTER 4 : RESULTS AND DISCUSSION

4.1 Calibration of flow rate

Figure 4.1 showed the curve according to the effluent and the pump speed. The speed of the pump was maintained by remain the influent constantly 1 cm above the MIRHA inside the column. For different bed height, the flowrate of the influent also different. After the result of the effluent obtained, graph Flowrate versus Pump Speed is plotted. From the graph, we can see that, as the pump speed increased, the total effluent from the column also increase.

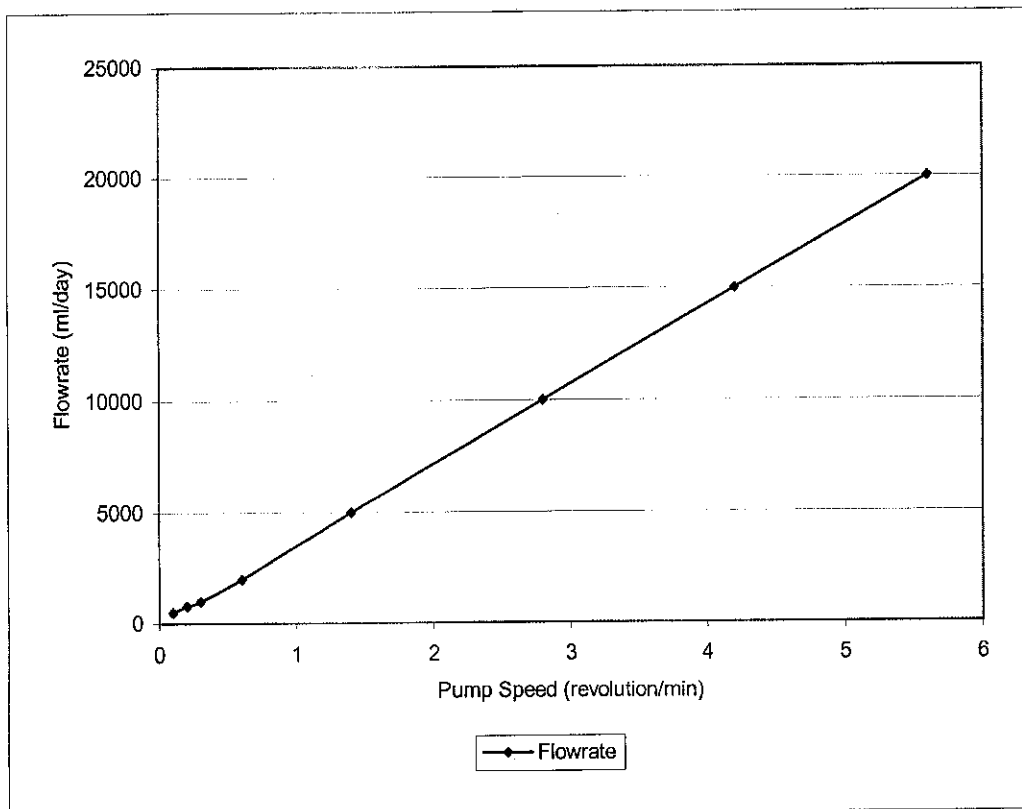


Figure 4.1 : Graph Flowrate vs Pump Speed

4.2 Adsorption Curve

4.2.1 Breakthrough curve for adsorption of Zinc

In order to examine the effect of different bed height of MIRHA on zinc solution, the experiment were done at bed height of 5, 10 and 15 cm. Figure 4.2(a) showed the breakthrough curve using a plot of dimensionless concentration (C/C_0) versus time (t).

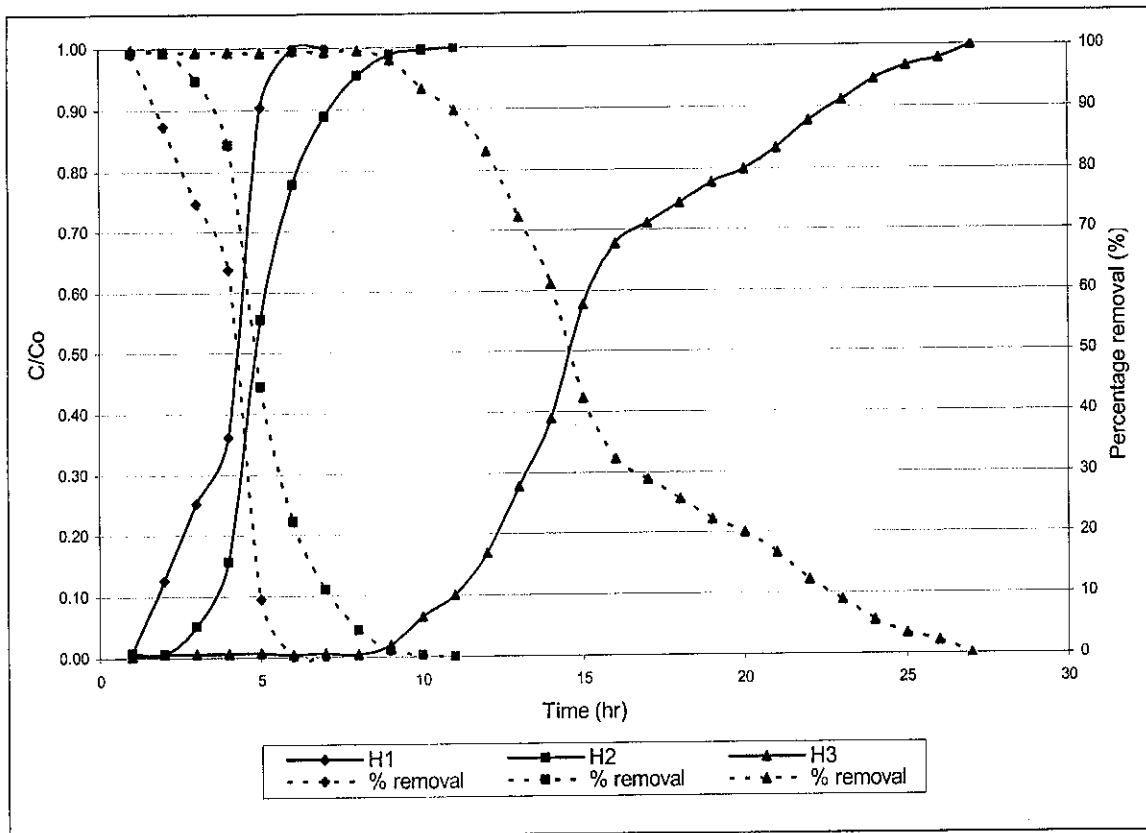


Figure 4.2(a) : Breakthrough curve for Zinc at different bed height ($C_0 = 9.4\text{mg/L}$)

As shown in Figure 4.2(a), with an increase of the bed height of the MIRHA, the breakthrough shifted from left to right, which indicated that the adsorption time increases as the bed height increase. The same concentration of effluent (C) with the influent (C_0) obtained at the end of the experiment. The initial percentage removal also shows that 100 % of the Zinc was removed by the MIRHA. It indicates that the MIRHA in the column were adsorbing the zinc.

4.2.2 Breakthrough curve for adsorption of Copper

Figure 4.2(b) showed the effect of Copper on the breakthrough curve using a plot of dimensionless concentration (C/C_0) versus time (t).

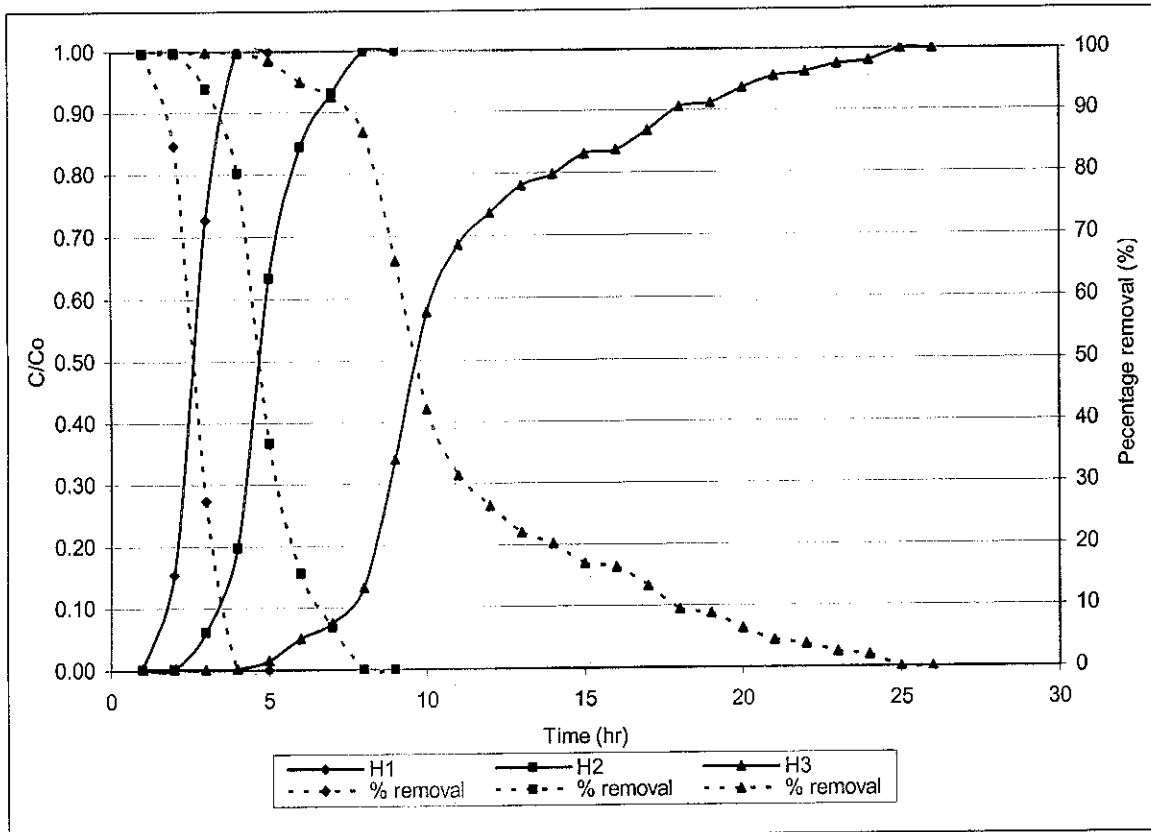


Figure 4.2(b) : Breakthrough curve for Copper at different bed height ($C_0 = 16.1$ mg/L)

Refer to Figure 4.2(b), the breakthrough also shifted from left to right, which indicated that the adsorption time increases as the bed height increase and the same concentration of C with C_0 obtained at the end of the experiment. The initial percentage removal also shows that 100 % of the Copper was removed by the MIRHA indicates that the MIRHA in the column were adsorbing the Copper.

It was seen from Figure 4.2(b) that breakthrough curves occurred faster than the Zinc. Breakthrough time for reaching C_0 was about 2 hours earlier than the previous.

4.2.3 Breakthrough curve for adsorption of Iron

Figure 4.2(c) showed the effect of Iron on the breakthrough curve using a plot of dimensionless concentration (C/C_0) versus time (t).

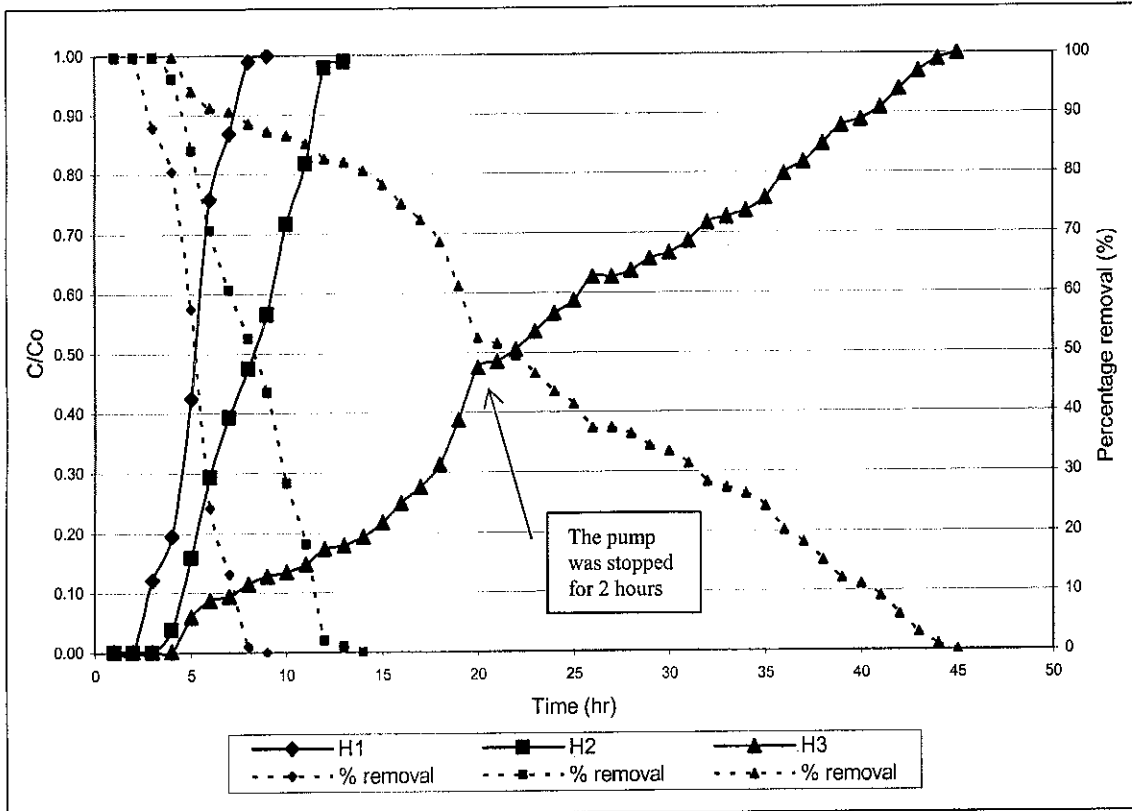


Figure 4.2(c): Breakthrough curve for Iron at different bed height ($C_0 = 9.9 \text{ mg/L}$)

As shown in Figure 4.2(c), with the increased of the bed height of the MIRHA, the breakthrough shifted from left to right, which indicated that the adsorption time increases as the bed height increase. The same concentration of effluent (C) with the influent (C_0) obtained at the end of the experiment. The initial percentage removal also shows that 100 % of the Iron was removed by the MIRHA indicates that the MIRHA in the column were adsorbing the Iron.

. By referring to Figure 4.2(a), 4.2(b) and 4.2(c) respectively, shows that the breakthrough occur for all heavy metal since the initial concentration of Zinc, Copper and Iron were the same as the effluent at certain time.

Different types of heavy metal have different time of breakthrough. Referring to Figure 4.2(a), we can see that for bed height of 5 cm, the breakthrough occur between 4 to 5 hours of the experiment while for 10 cm of bed height, the breakthrough occur between 8 to 10 hours of the experiment. But for the bed height of 15 cm, the breakthrough takes longer time compare to the previous that is between 16 to 27 hours of the experiment.

From experiment, it was seen that as the bed increased, the zinc, copper and iron had more time contact with the rice husk that resulted 100 % of removal for different period of time and decreasing as the time increases. The higher the bed column resulted in a decrease in the solute concentration in the effluent at the same time. Higher uptake was observed at the highest bed height due to an increase in the surface area of the adsorbent, which provided more binding sites for the sorption to occur. (Vijayaraghavan et al., 2004)

From the breakthrough result obtained, by comparing the graph after 5 hours, the earliest breakthrough achieved by the copper and the latest were the iron. From the result also, 15 cm bed height of MIRHA were the most effiecient bed height in the adsorption process because of the high degree of contact with the heavy metal and the adsorbent.

4.2.4 Breakthrough curve for adsorption of different heavy metal

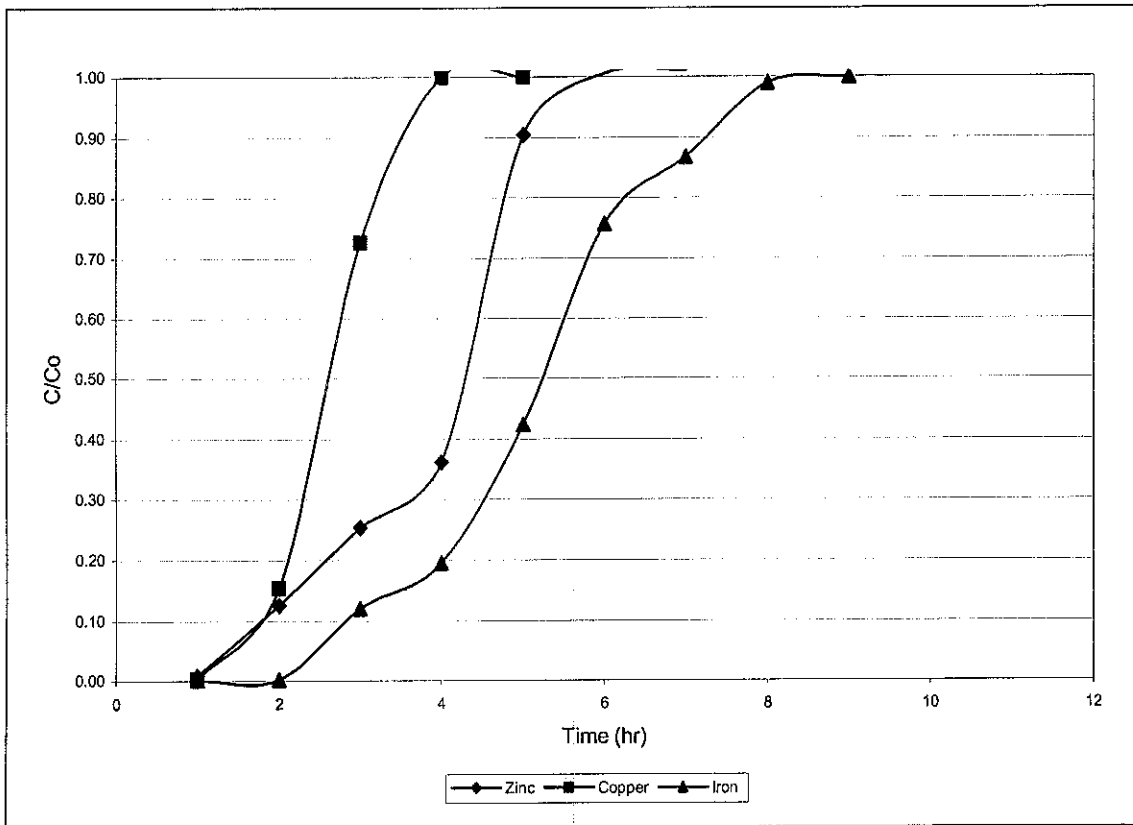


Figure 4.3(a): Breakthrough curve of heavy metal at bed height 5 cm

Referring to Figure 4.3(a), shows that the effect of the MIRHA at different types of heavy metal. It shows that Copper has the earliest time where the heavy metal was detected at the effluent followed by Zinc and Iron.

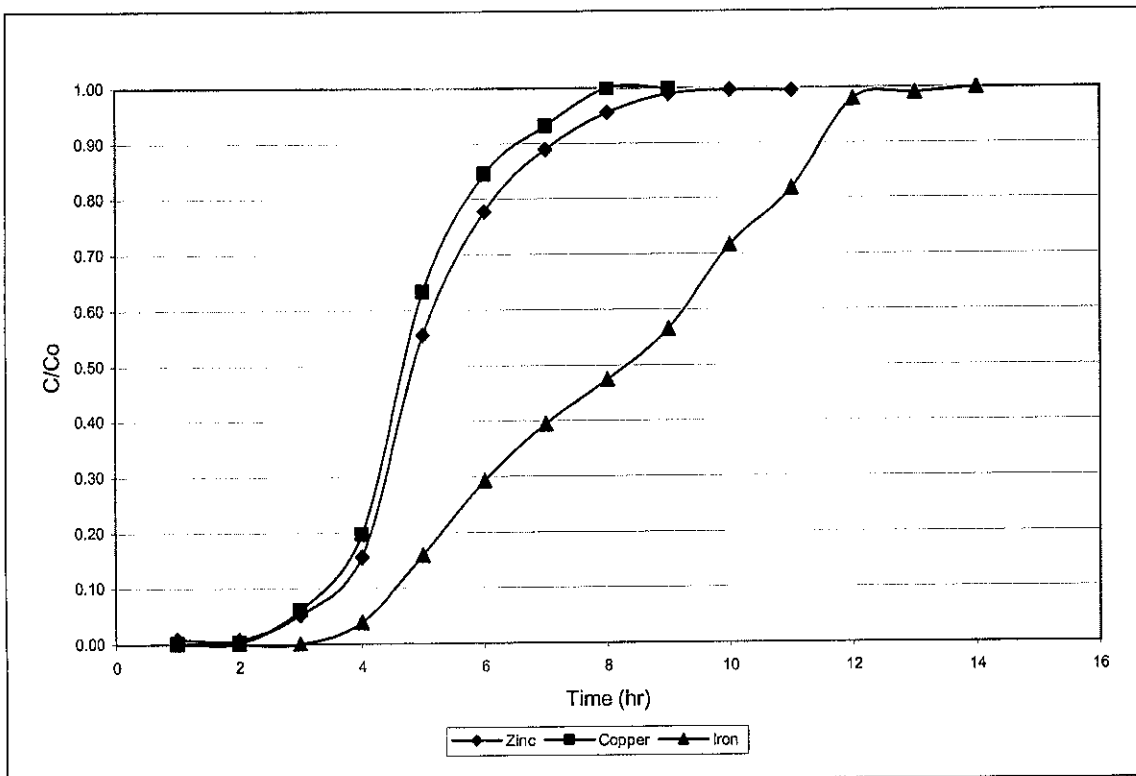


Figure 4.3(b): Breakthrough curve of heavy metal at bed height 10 cm

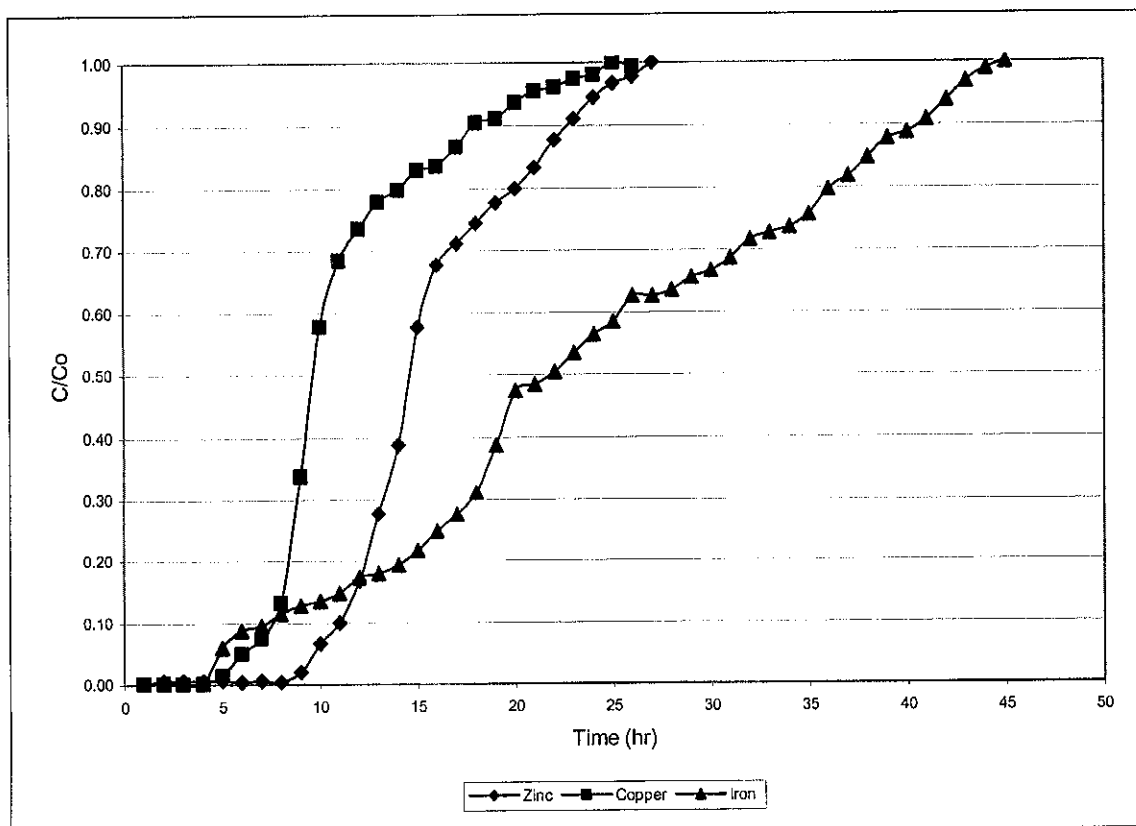


Figure 4.3(c): Breakthrough curve of heavy metal at bed height 15 cm

Referring to Figure 4.3(b) and Figure 4.3(c), shows that the effect of the MIRHA at different types of heavy metal. It also shows that the Copper has the earliest time where the heavy metal was detected at the effluent followed by Zinc and Iron.

From the graph obtained, we can see that, different types of heavy metal has a different impact on the same bed height of the MIRHA. The MIRHA was adsorbing the Zinc, Copper and Iron at a different rate with the same bed height of the MIRHA.

4.3 Modeling of breakthrough curve

In order to describe the fixed-bed column behavior and to scale it up for industrial applications, three models, Thomas, Adams–Bohart and Yoon–Nelson were used to fit the experimental data in the column. Although linear least-square regressive analysis is often used to obtain the model parameters (Aksu and Gonen, 2004), non-linear regressive analysis is also adopted to determine the relative parameters [(Kumar and Sivanesan, 2007) and (Yan and Viraraghavan, 2001)].

4.3.1 Thomas Model

The column data were fitted to the Thomas model to determine the Thomas rate constant (k_{Th}) and maximum solid-phase concentration (q_0). The determined coefficients and relative constants were obtained using non-linear regression analysis according to Eq. (1) and the graph were plotted according to the types of heavy metal and the bed height.

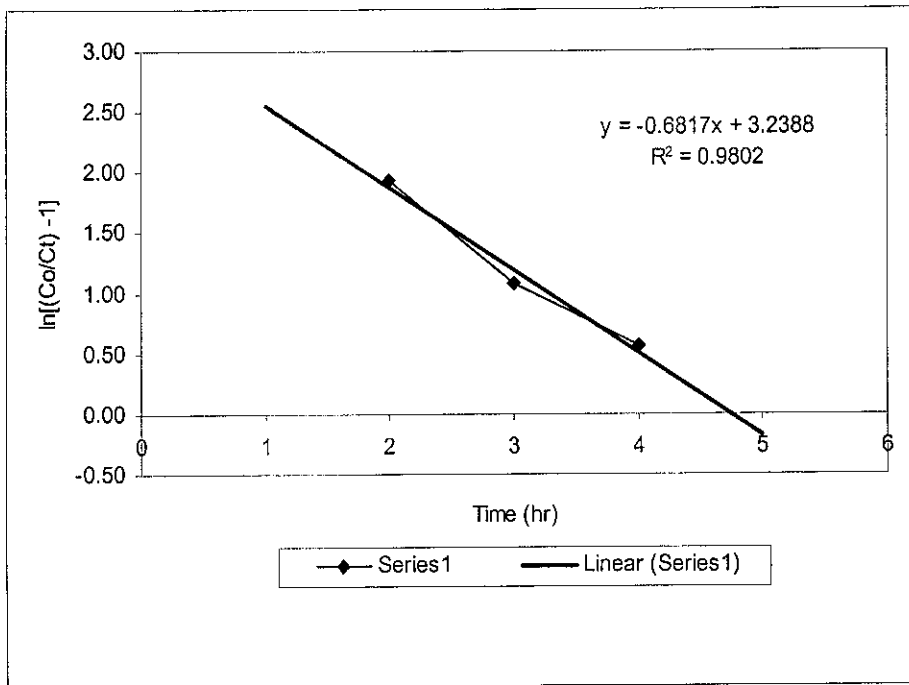


Figure 4.4(a) : Breakthrough curve obtained according to the Thomas Model
(Zinc, $z=5$ cm, $Co = 9.4$ mg/L)

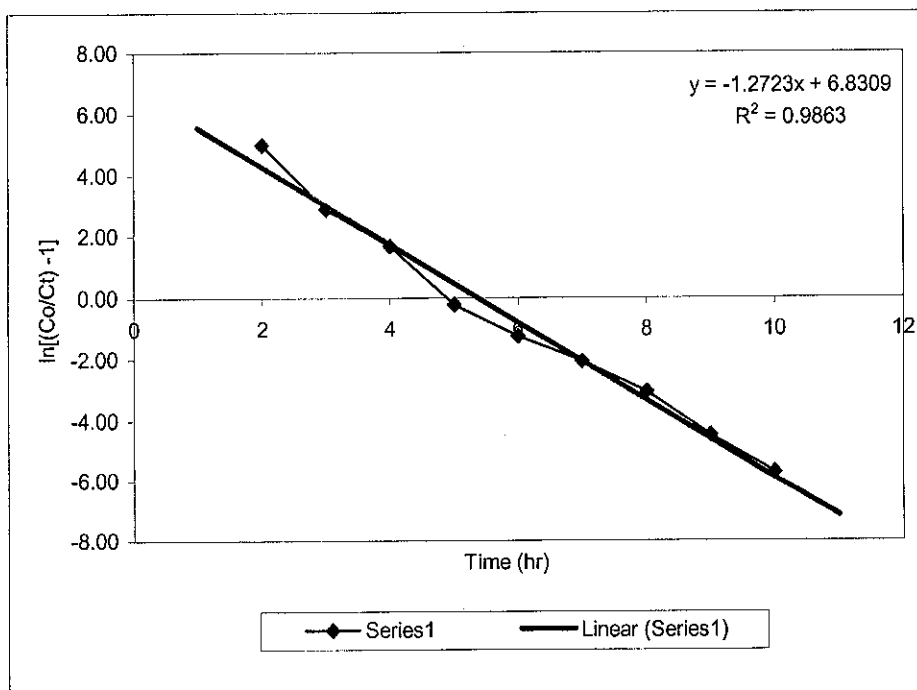


Figure 4.4(b) : Breakthrough curve obtained according to the Thomas Model
(Zinc, $z=10$ cm, $Co = 9.0$ mg/L)

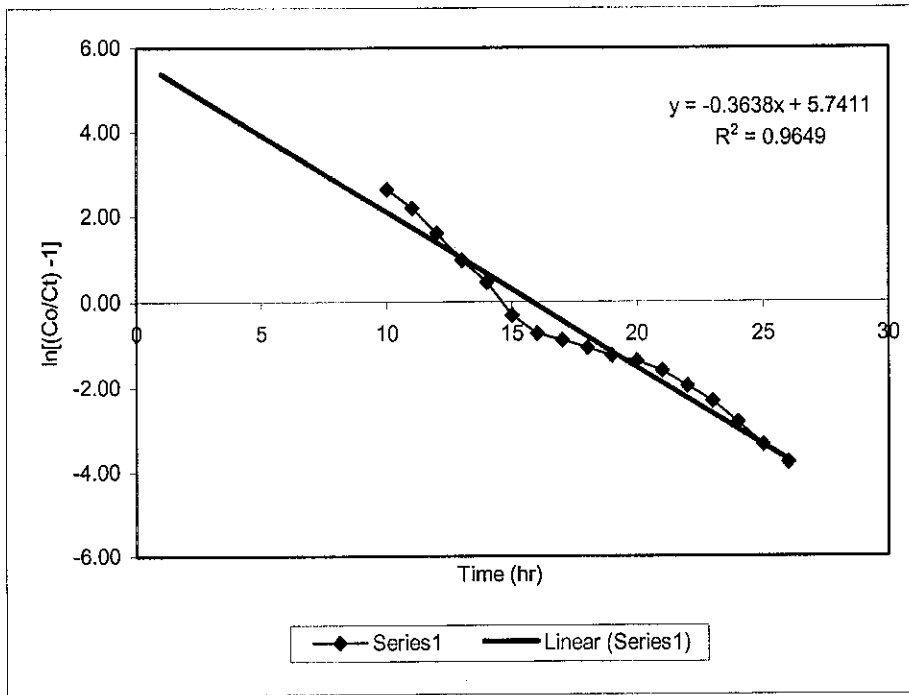


Figure 4.4(c) : Breakthrough curve obtained according to the Thomas Model
(Zinc, z=15 cm, Co = 9.0 mg/L)

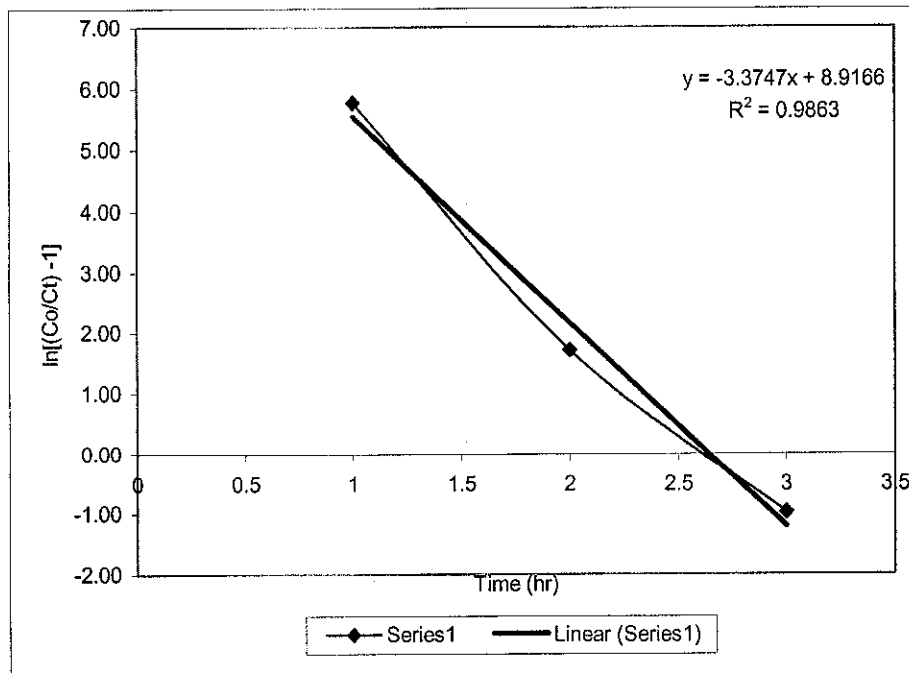


Figure 4.4(d) : Breakthrough curve obtained according to the Thomas Model
(Copper, z=5 cm, Co = 16.1 mg/L)

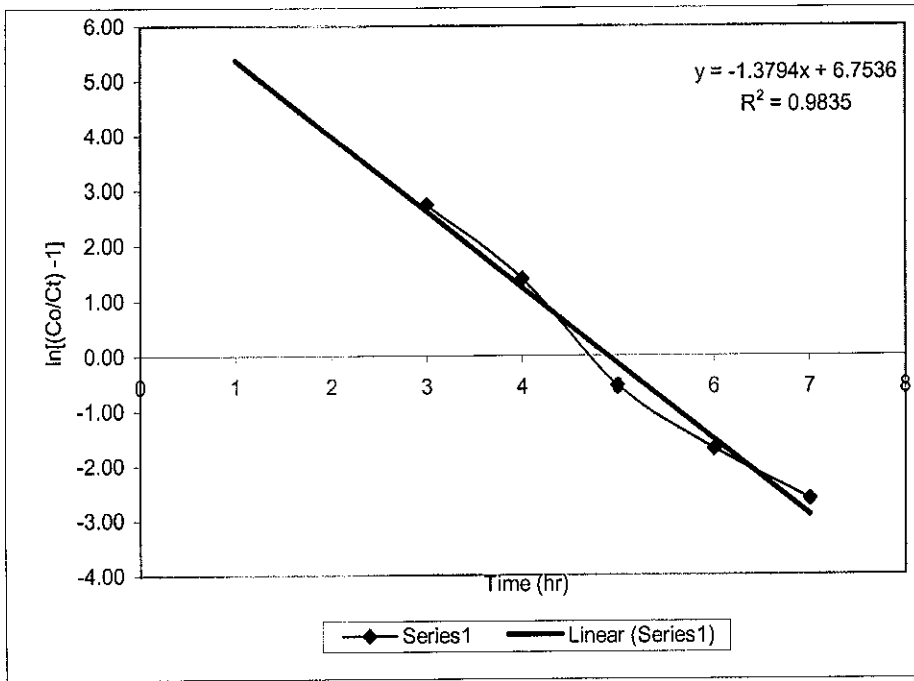


Figure 4.4(e) : Breakthrough curve obtained according to the Thomas Model
(Copper, z=10 cm, Co = 16.1 mg/L)

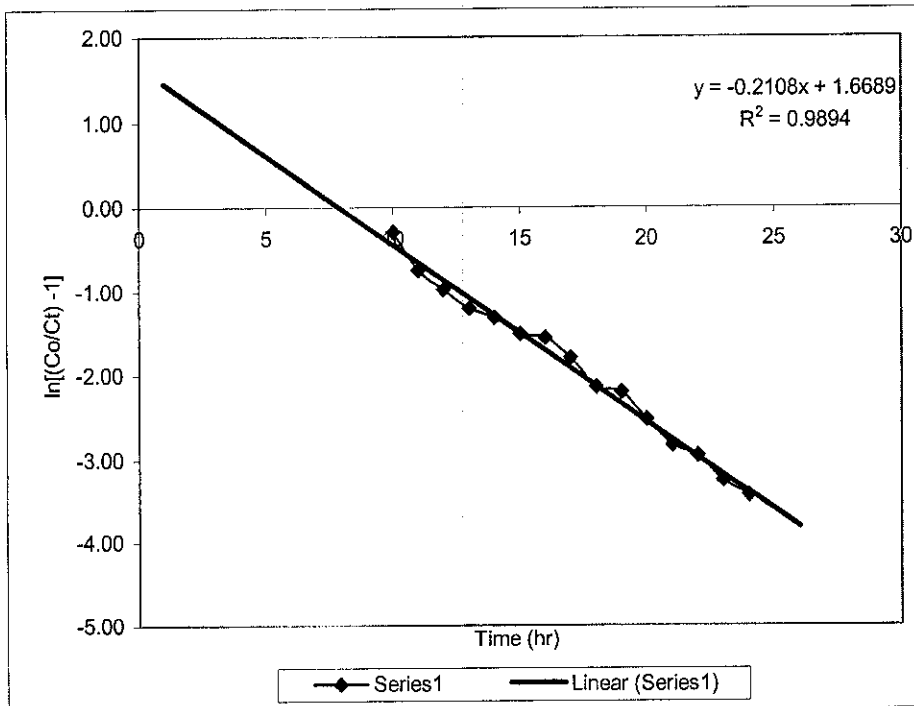


Figure 4.4(f) : Breakthrough curve obtained according to the Thomas Model
(Copper, z=15 cm, Co = 16.1 mg/L)

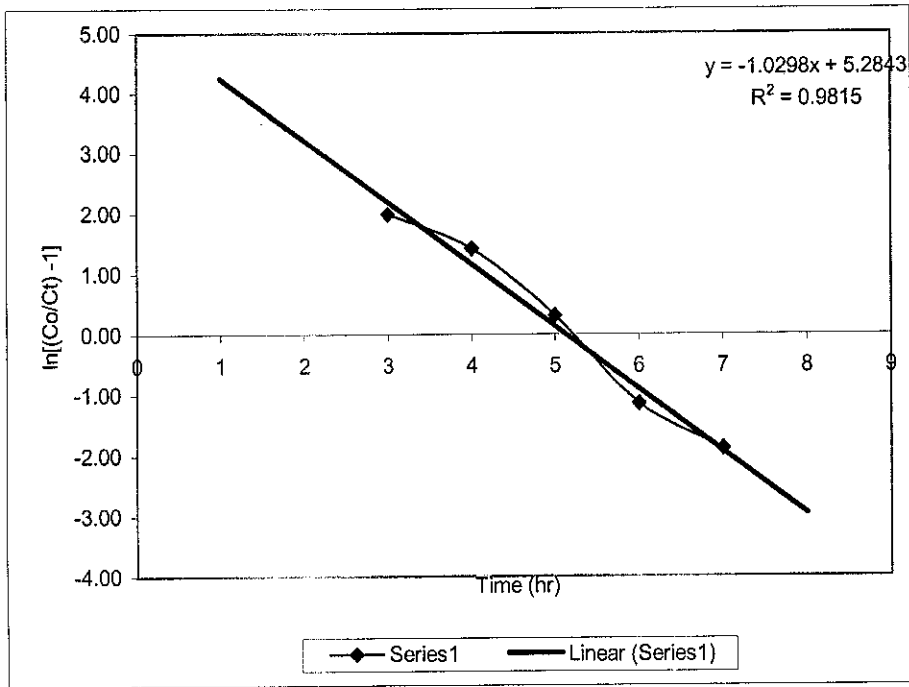


Figure 4.4(g) : Breakthrough curve obtained according to the Thomas Model
 (Iron, z=5 cm, Co = 9.9 mg/L)

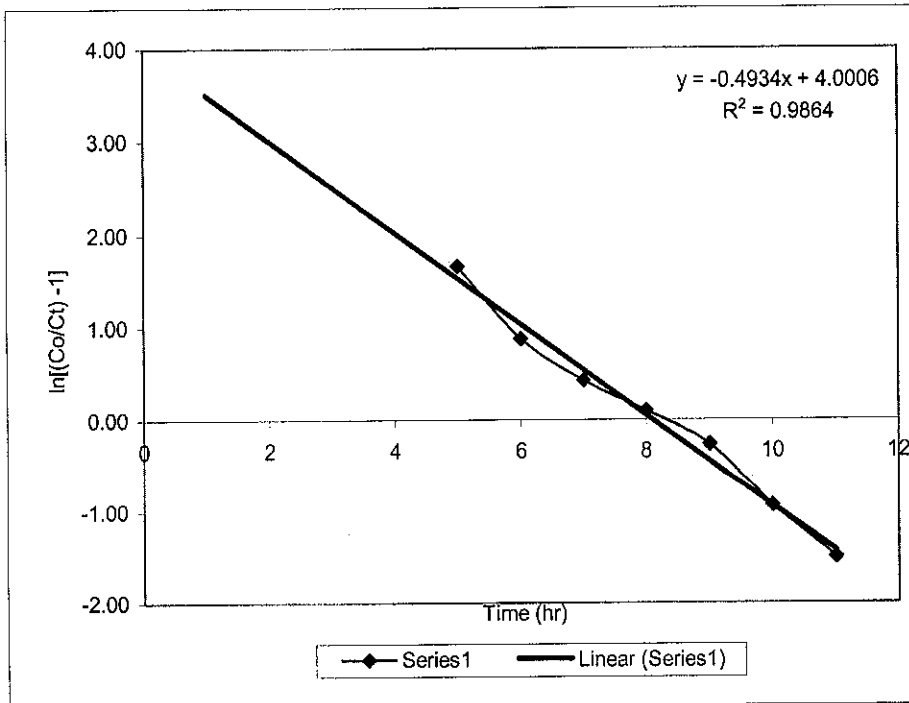


Figure 4.4(h) : Breakthrough curve obtained according to the Thomas Model
 (Iron, z=10 cm, Co = 9.9 mg/L)

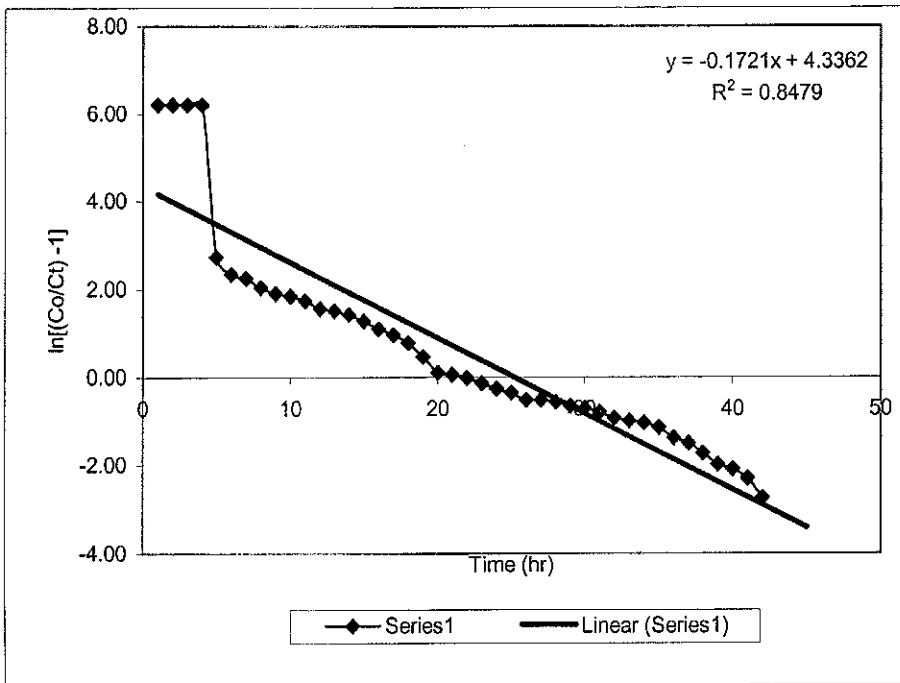


Figure 4.4(i) : Breakthrough curve obtained according to the Thomas Model
(Iron, $z=15$ cm, $Co = 9.9$ mg/L)

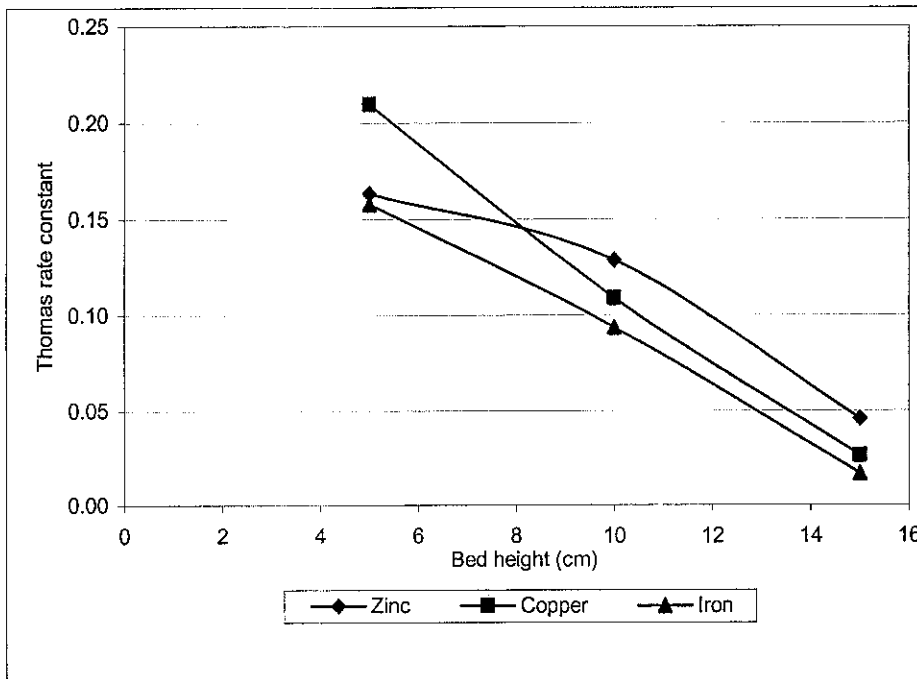


Figure 4.5(a) : Relationship between Thomas rate constant (k_{Th}) with bed height

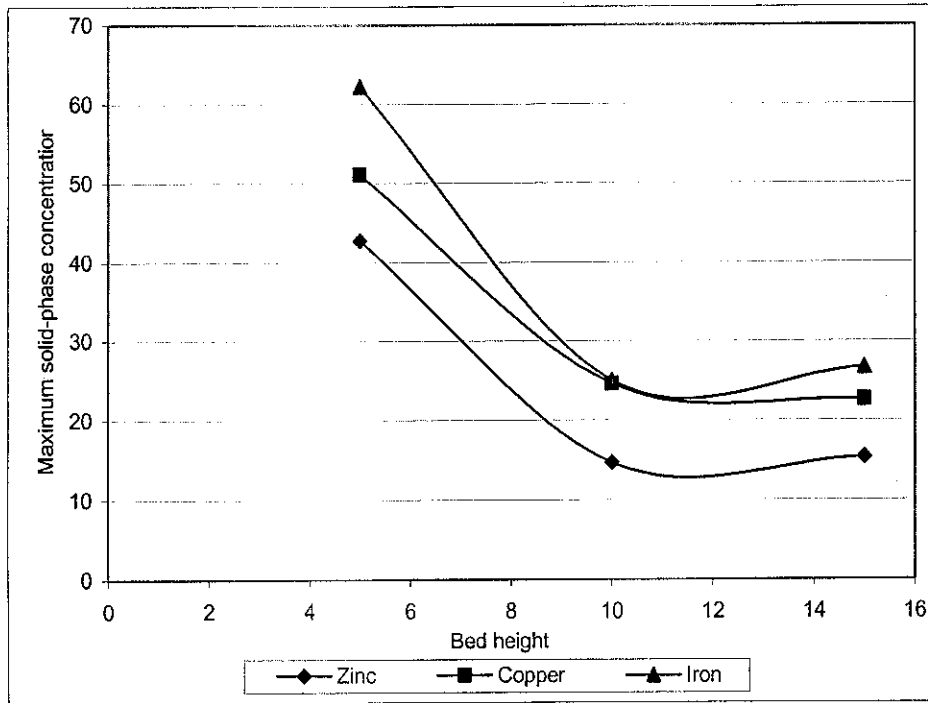


Figure 4.5(b) : Relationship between maximum solid-phase concentration (q_0) with bed height

From Table 4.1, it is seen that the values of determined coefficient (R^2) range from 0.8479 to 0.9894, where the values of R^2 are at optimum. So the relation of C_t/C_0 and t according to the Equation (1) is significant.

Table 4.1 : Thomas model parameters at different condition using non-linear regression analysis
Thomas Model

	C_0 (mg/L)	v (ml/min)	Z (cm)	K_{TH}	q_0	R^2
Zinc	9.40	24	5	0.164	42.803	0.9802
	9.00	13	10	0.129	14.671	0.9863
	9.00	6	15	0.046	15.339	0.9649
Copper	16.10	24	5	0.210	51.069	0.9863
	16.10	13	10	0.109	24.619	0.9835
	16.10	6	15	0.027	22.644	0.9894
Iron	9.90	24	5	0.158	62.253	0.9815
	9.90	13	10	0.094	25.082	0.9864
	9.90	6	15	0.017	26.703	0.8479

From Table 4.1, as the influent concentration increased, the value of q_0 and K_{TH} decreased. The reason is that the driving force for biosorption is the difference between the heavy metal on the adsorbent and the heavy metal in the solution (Aksu and Gonen, 2004). Thus, the high concentration of the heavy metal resulting the better contact of the heavy metal with the adsorbent. The bed capacity q_0 and the Thomas constant K_{TH} decreased with the flowrate decreasing. With the bed height increased, the value of q_0 decreased. So the heavy metal have slow contact time with the adsorbent resulting high efficiency of heavy metal removal.

Referring to the graph obtained from Equation (1), shows that the adsorption rate were linear up to 50% breakthrough according to the Thomas model. Even though the model only gave a general prediction of the experimental data, there was a good comparison between the experimental and predicted normalized concentration values at experimental conditions. The Thomas model shows that the external and internal diffusion will not be the limiting steps and it is suitable for adsorption process.

4.3.2 The Adams-Bohart model

The Adams–Bohart adsorption model was applied to experimental data for the description of the initial part of the breakthrough curve. This approach was focused on the estimation of characteristic parameters, such as maximum adsorption capacity (N_0) and kinetic constant (k_{AB}) from Adams–Bohart model.

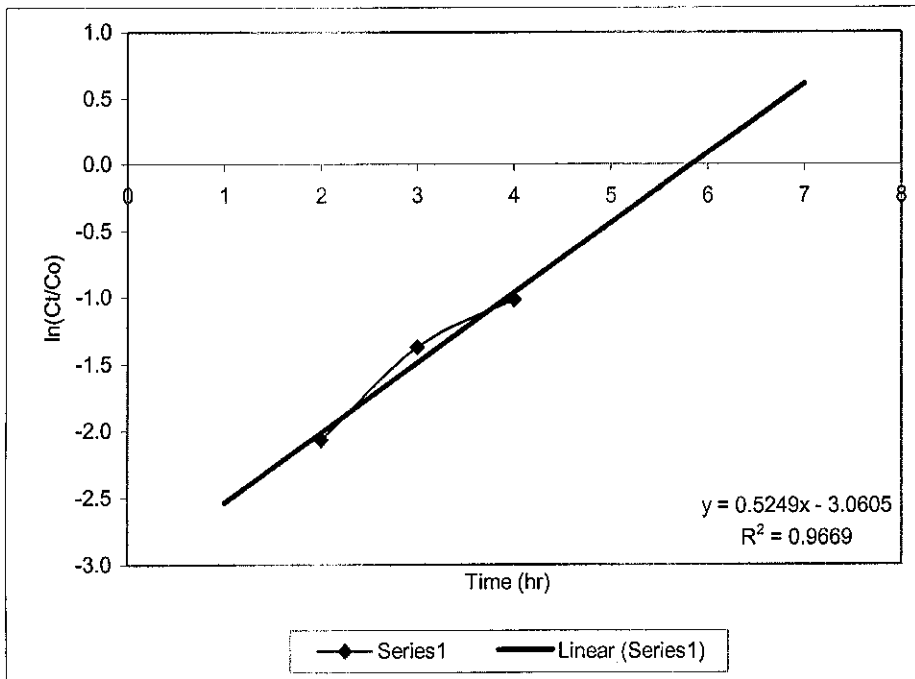


Figure 4.6(a) : Breakthrough curve obtained according to the Adams-Bohart Model
(Zinc, z=5 cm, Co = 9.4 mg/L)

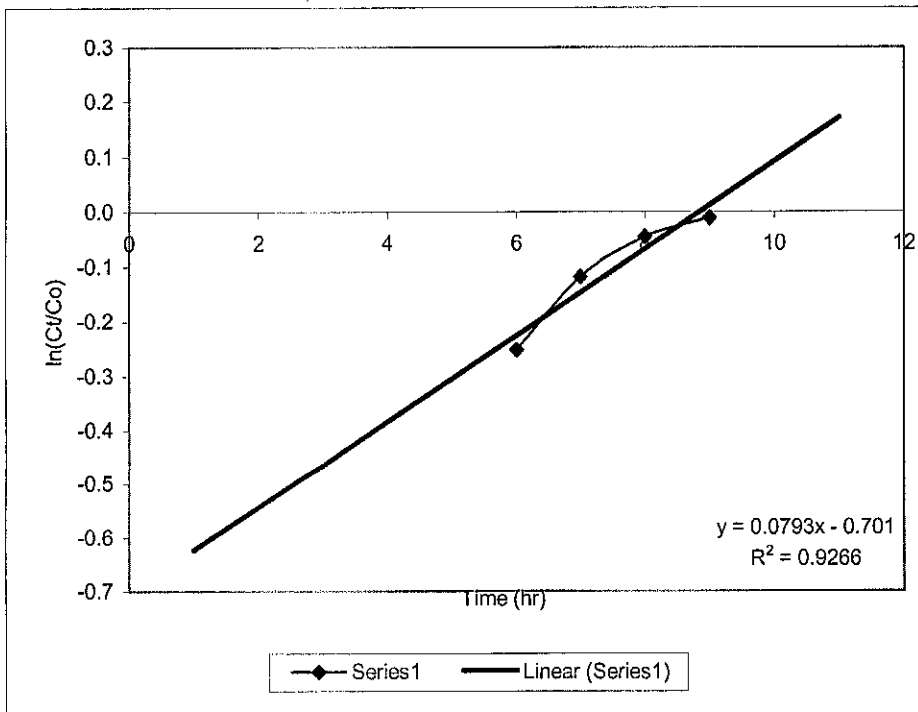


Figure 4.6(b) : Breakthrough curve obtained according to the Adams-Bohart Model
(Zinc, z=10 cm, Co = 9.0 mg/L)

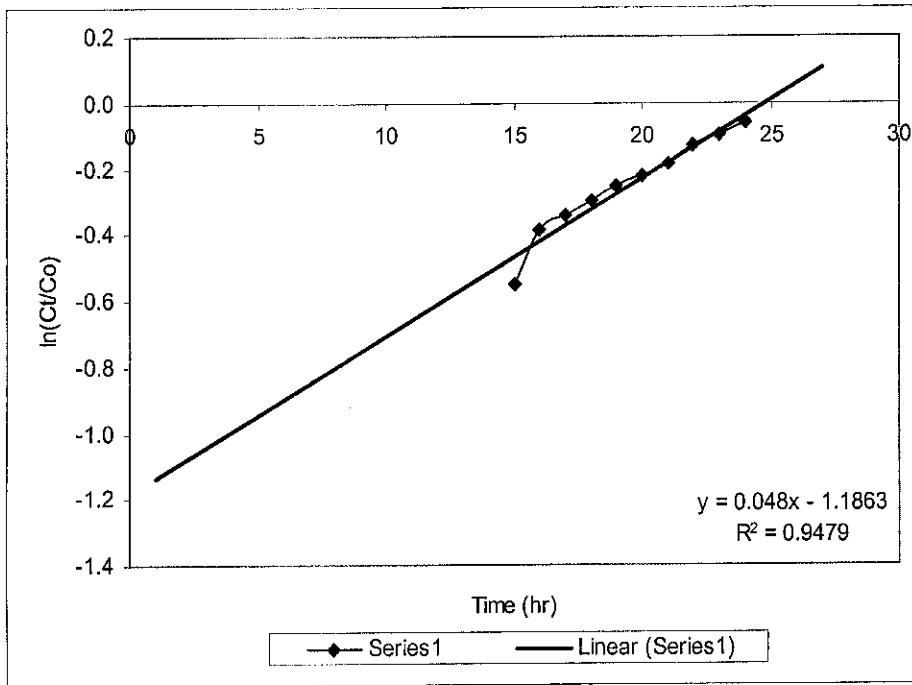


Figure 4.6(c) : Breakthrough curve obtained according to the Adams-Bohart Model
(Zinc, $z=15$ cm, $C_o = 9.4$ mg/L)

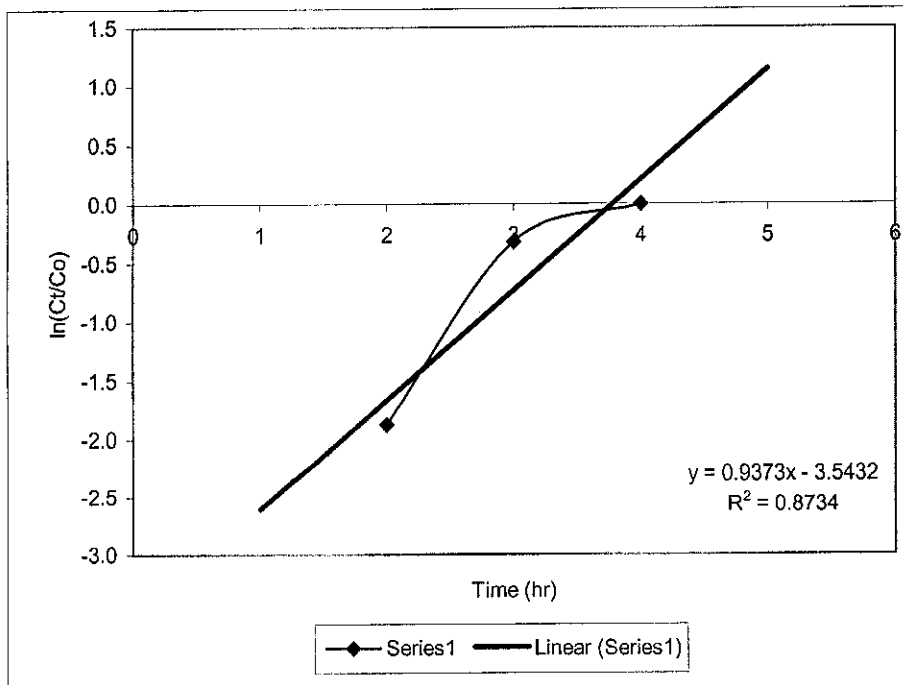


Figure 4.6(d) : Breakthrough curve obtained according to the Adams-Bohart Model
(Copper, $z=5$ cm, $C_o = 16.1$ mg/L)

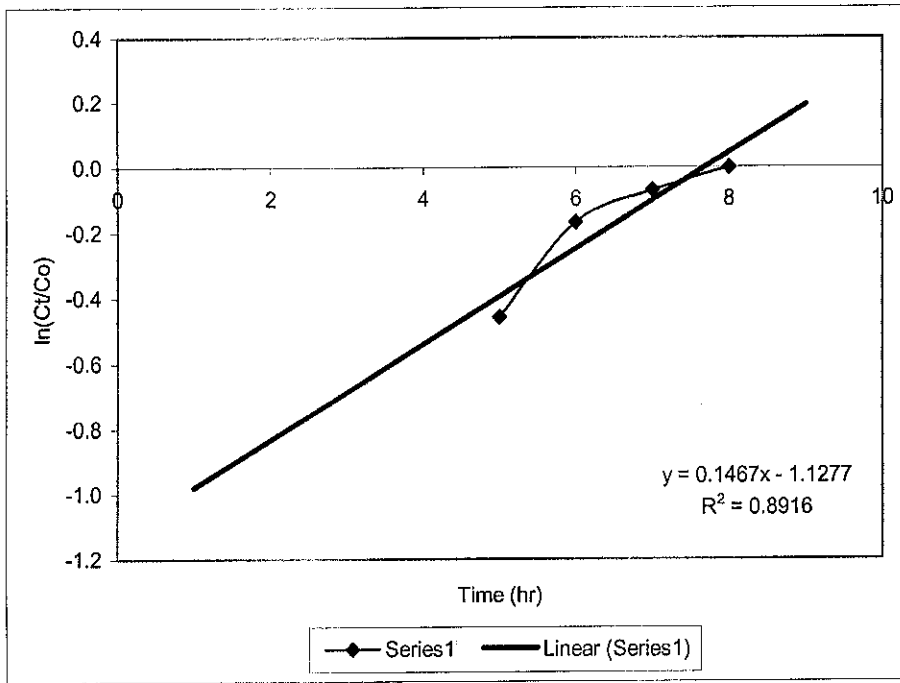


Figure 4.6(e) : Breakthrough curve obtained according to the Adams-Bohart Model
 (Copper, z=10 cm, Co = 16.1 mg/L)

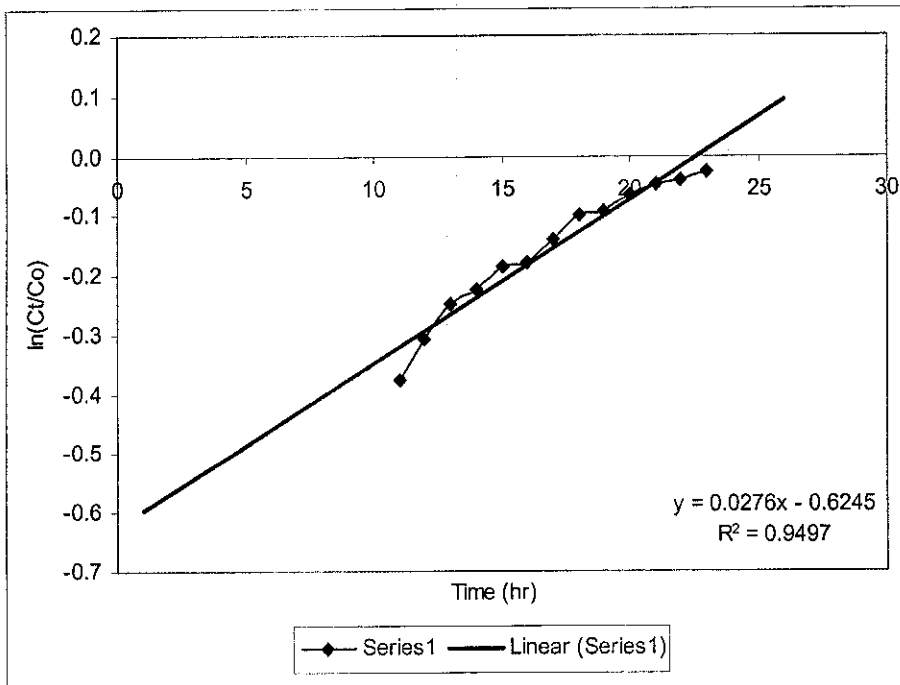


Figure 4.6(f) : Breakthrough curve obtained according to the Adams-Bohart Model
 (Copper, z=15 cm, Co = 16.1 mg/L)

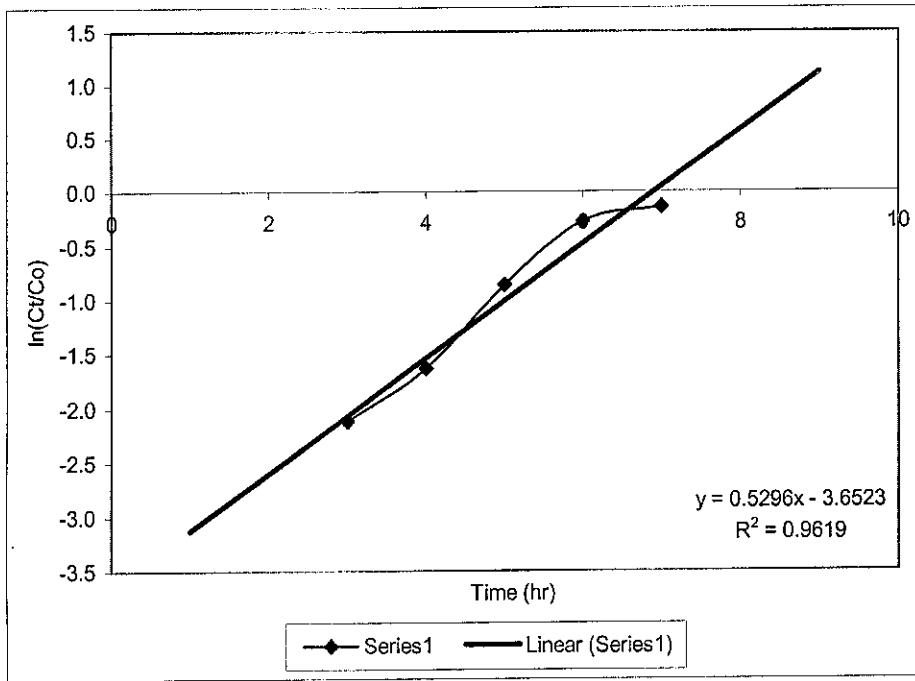


Figure 4.6(g) : Breakthrough curve obtained according to the Adams-Bohart Model
 (Iron, $z=5$ cm, $C_o = 9.9$ mg/L)

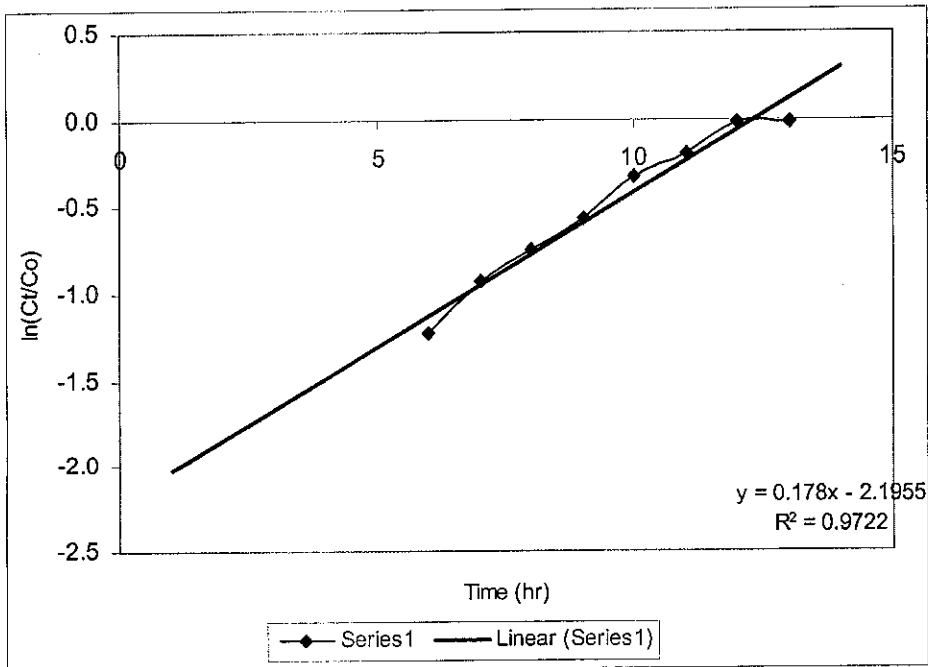


Figure 4.6(h) : Breakthrough curve obtained according to the Adams-Bohart Model
 (Iron, $z=10$ cm, $C_o = 9.9$ mg/L)

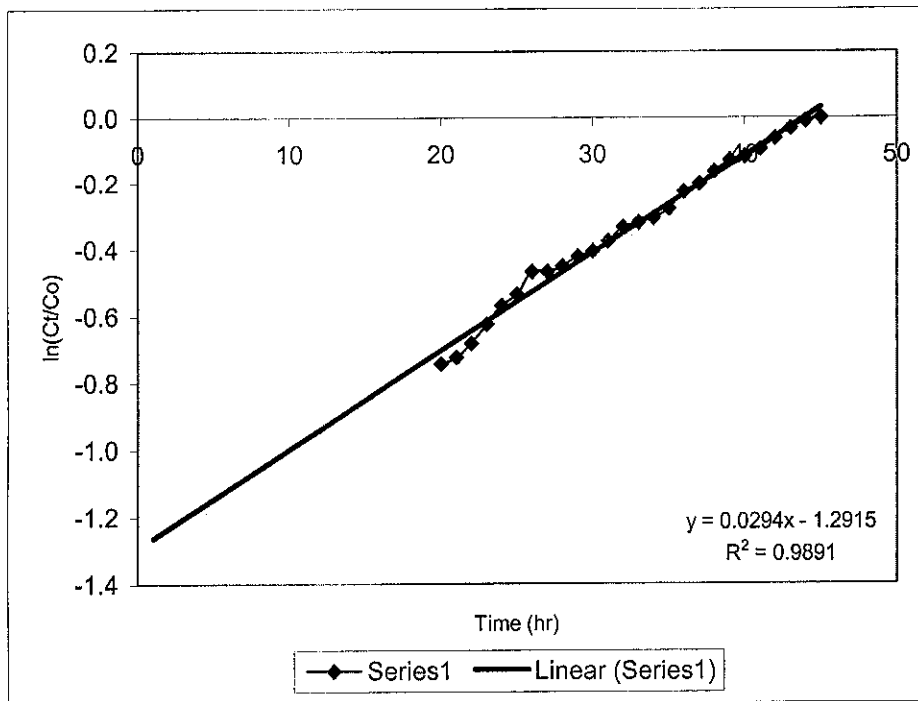


Figure 4.6(i) : Breakthrough curve obtained according to the Adams-Bohart Model
(Iron, $z=15$ cm, $C_0 = 9.9$ mg/L)

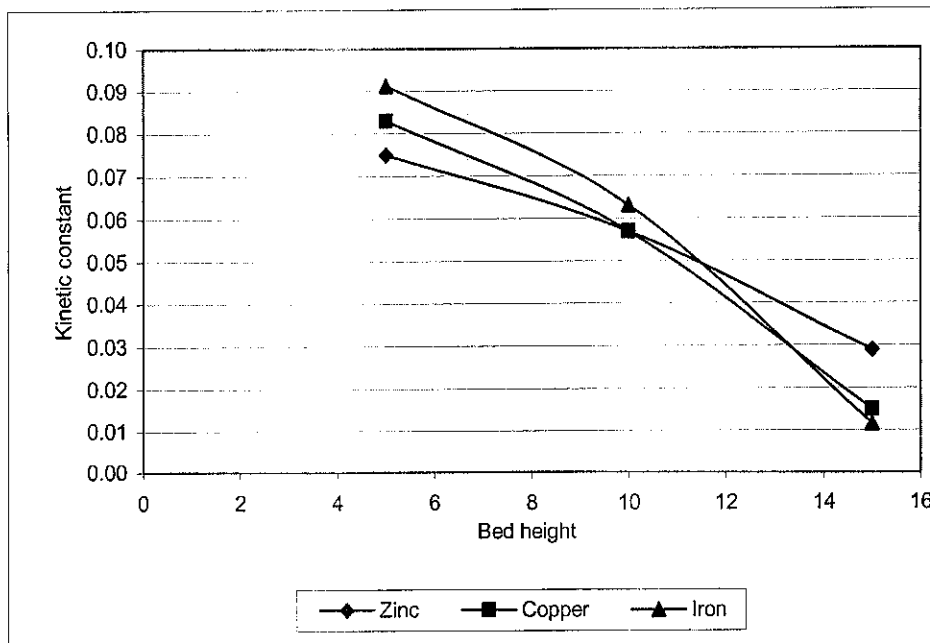


Figure 4.7(a) : Relationship between kinetic constant (k_{AB}) with bed height

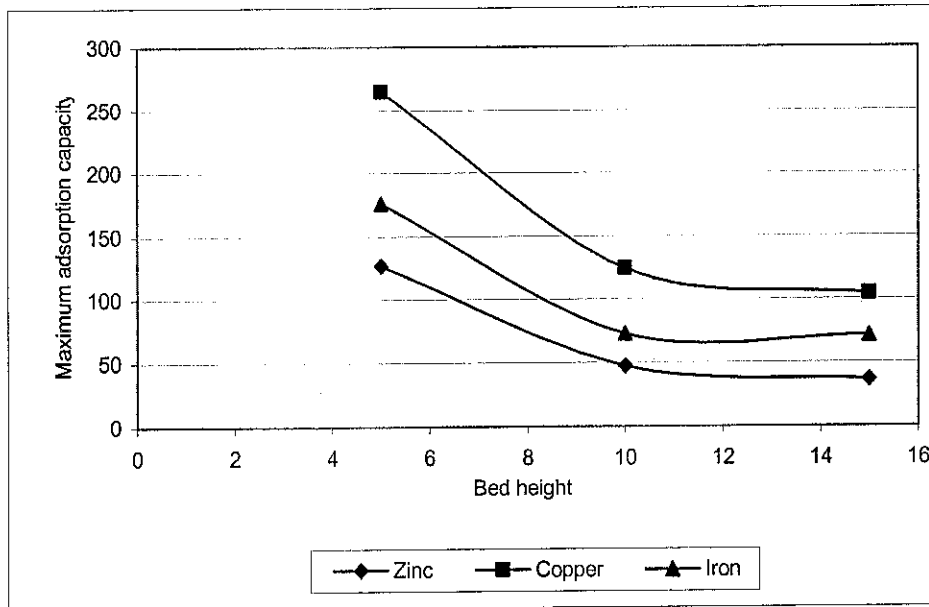


Figure 4.7(b) : Relationship between maximum adsorption capacity (N_0) with bed height

After applying Equation (2) to the experimental data, the parameters were obtained for the relative concentration region up to 50% breakthrough, for all breakthrough curves using non-linear. For all breakthrough curves, respective values of N_0 , and k_{AB} were calculated and presented in Table 4.2.

Table 4.2 : Adams-Bohart parameters at different conditions using non-linear regression analysis (up 50%)

Adams-Bohart Model

	C_0 (mg/L)	v (ml/min)	Z (cm)	K_{AB}	N_0	R^2
Zinc	9.40	24	5	0.075	126.951	0.9669
	9.00	13	10	0.057	47.524	0.9266
	9.00	6	15	0.029	36.391	0.9479
Copper	16.10	24	5	0.083	265.098	0.8734
	16.10	13	10	0.057	124.762	0.8916
	16.10	6	15	0.015	104.201	0.9497
Iron	9.90	24	5	0.091	175.857	0.9619
	9.90	13	10	0.063	73.03	0.9122
	9.90	6	15	0.012	71.572	0.9891

The predicted curves suggested that the Adams-Bohart model will be valid for the relative concentration region up to 50% where the graph is linear within the region.

4.3.3 The Yoon-Nelson model

A simple theoretical model developed by Yoon–Nelson was applied to investigate the breakthrough behavior of heavy metal on rice husk. So the values of the rate constant (k_{YN}) and the time required for 50% breakthrough (τ) could be obtained using non-linear regressive analysis from Equation (3).

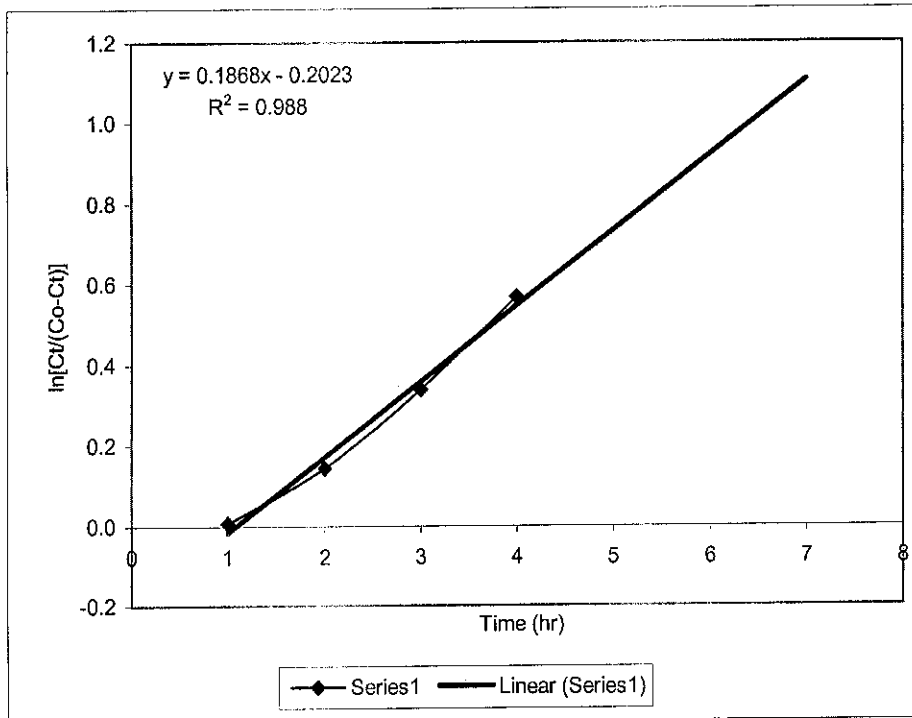


Figure 4.8(a) : Breakthrough curve obtained according to the Yoon-Nelson Model
(Zinc, $z=5$ cm, $Co = 9.4$ mg/L)

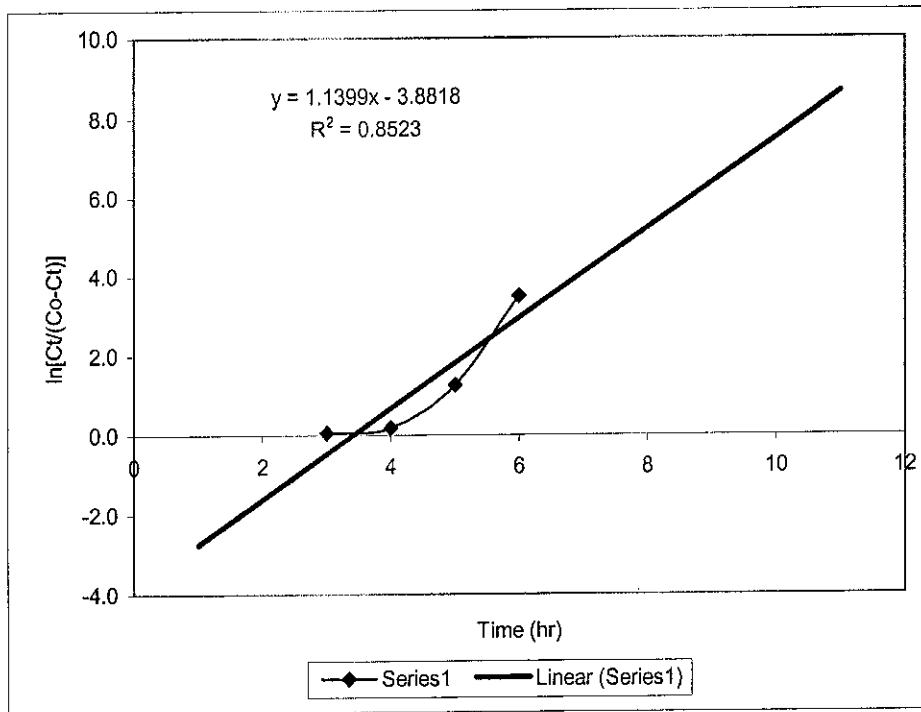


Figure 4.8(b) : Breakthrough curve obtained according to the Yoon-Nelson Model
(Zinc, $z=10$ cm, $Co = 9.0$ mg/L)

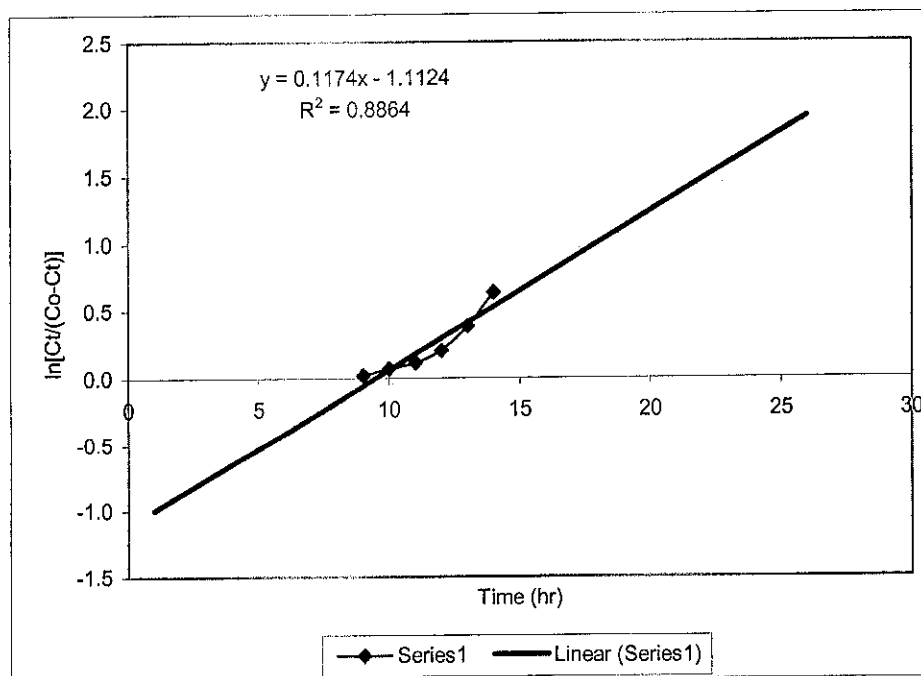


Figure 4.8(c) : Breakthrough curve obtained according to the Yoon-Nelson Model
(Zinc, $z=15$ cm, $Co = 9.0$ mg/L)

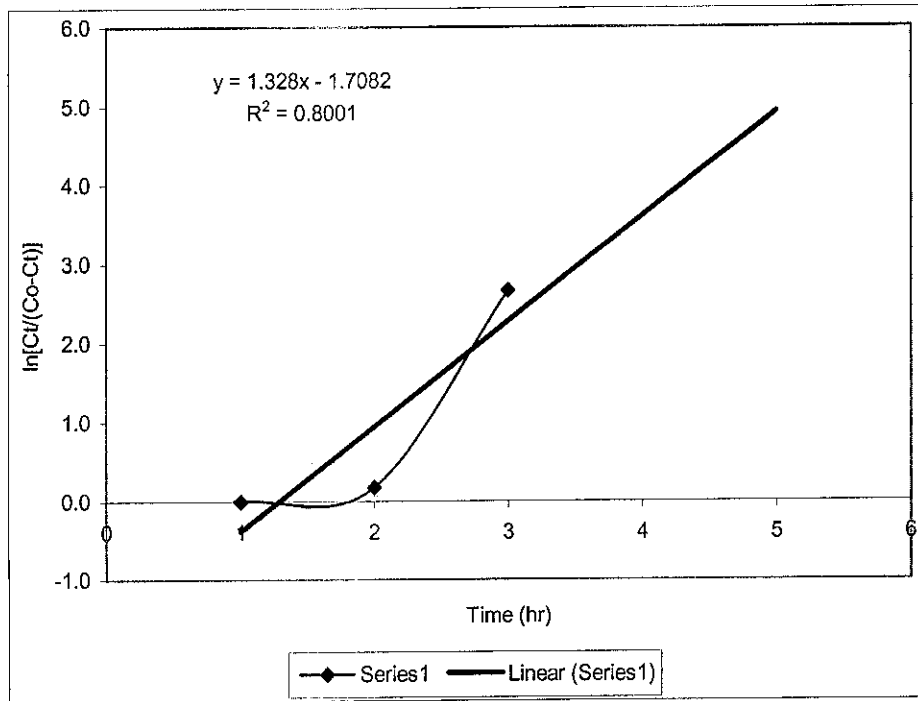


Figure 4.8(d) : Breakthrough curve obtained according to the Yoon-Nelson Model
(Copper, $z=5$ cm, $C_o = 16.1$ mg/L)

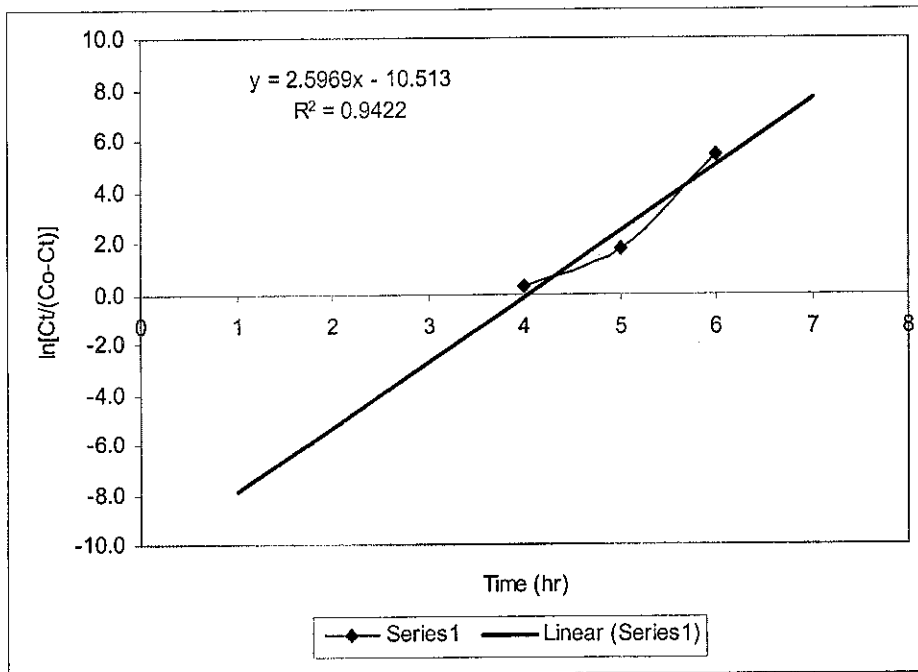


Figure 4.8(e) : Breakthrough curve obtained according to the Yoon-Nelson Model
(Copper, $z=10$ cm, $C_o = 16.1$ mg/L)

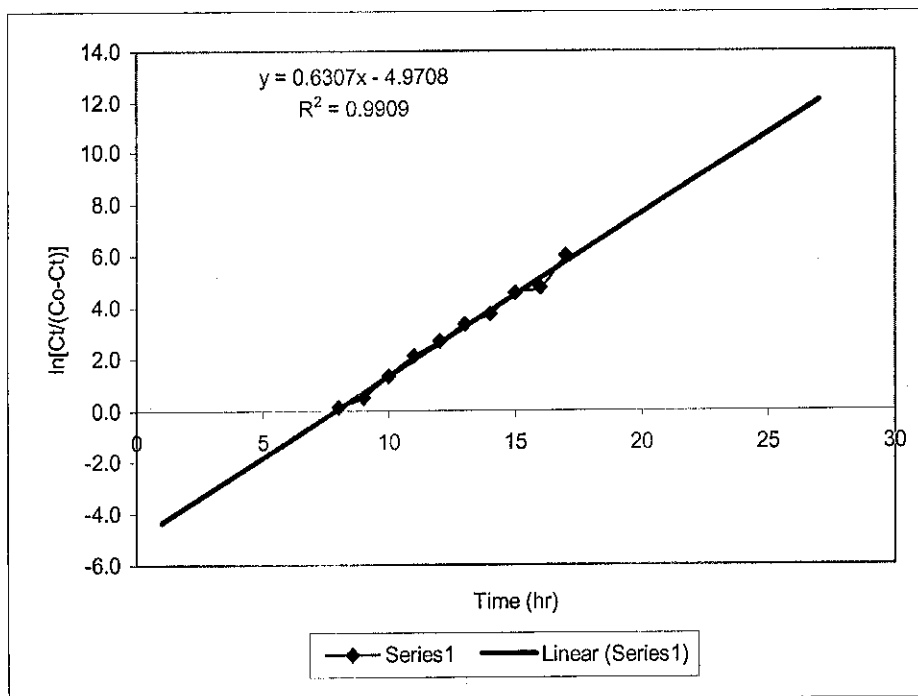


Figure 4.8(f) : Breakthrough curve obtained according to the Yoon-Nelson Model
(Copper, $z=15$ cm, $Co = 16.1$ mg/L)

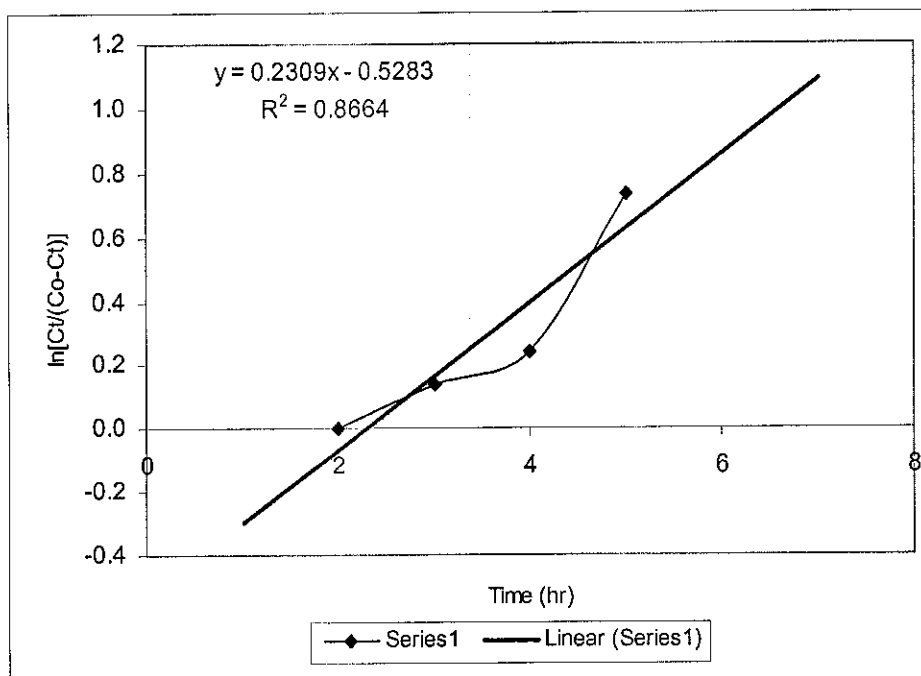


Figure 4.8(g) : Breakthrough curve obtained according to the Yoon-Nelson Model
(Iron, $z=5$ cm, $Co = 9.9$ mg/L)

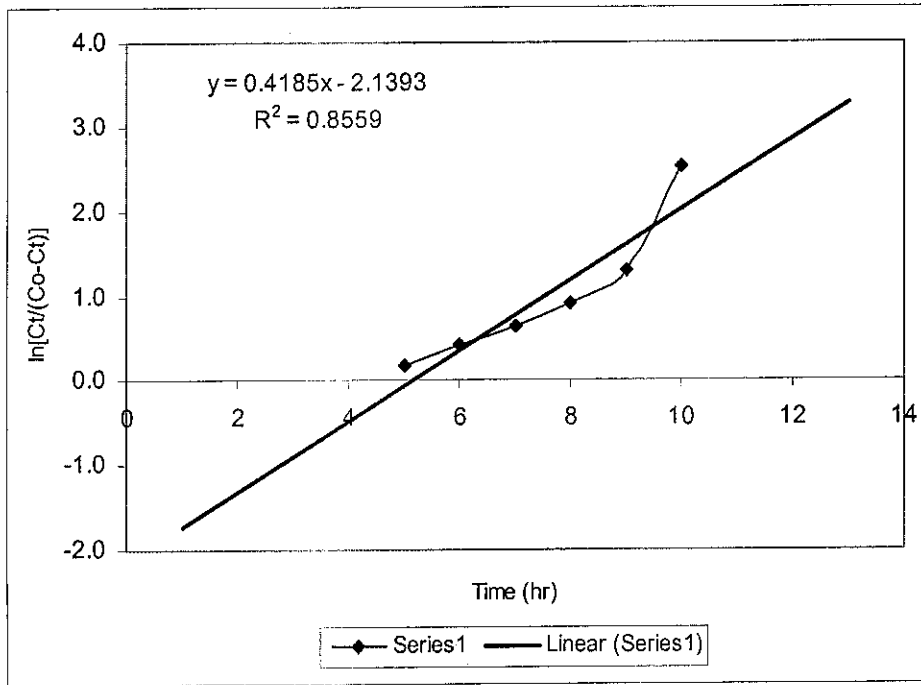


Figure 4.8(h) : Breakthrough curve obtained according to the Yoon-Nelson Model
(Iron, $z=10$ cm, $Co = 9.9$ mg/L)

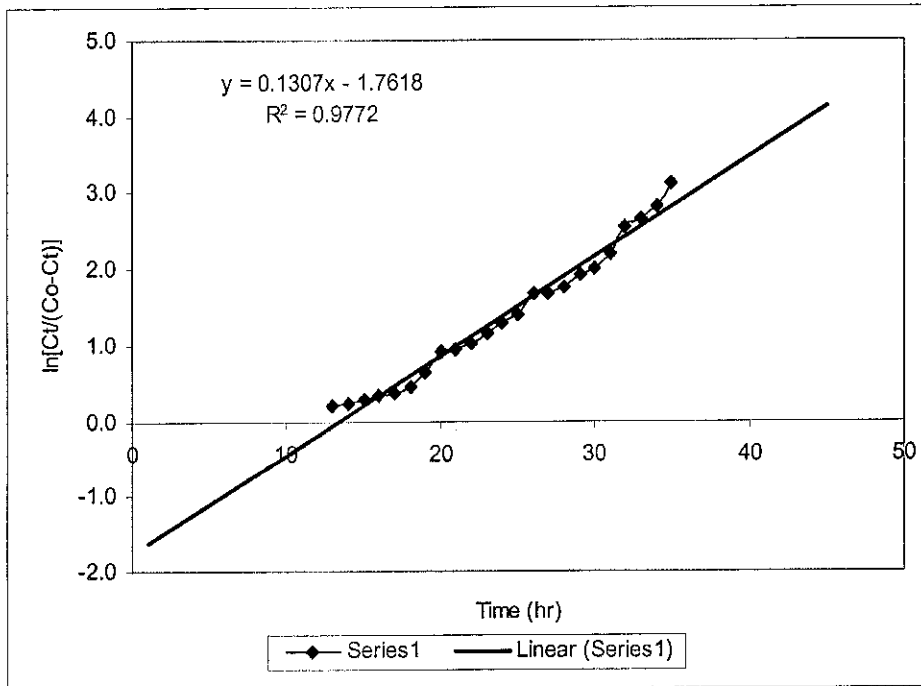


Figure 4.8(i) : Breakthrough curve obtained according to the Yoon-Nelson Model
(Iron, $z=15$ cm, $Co = 9.9$ mg/L)

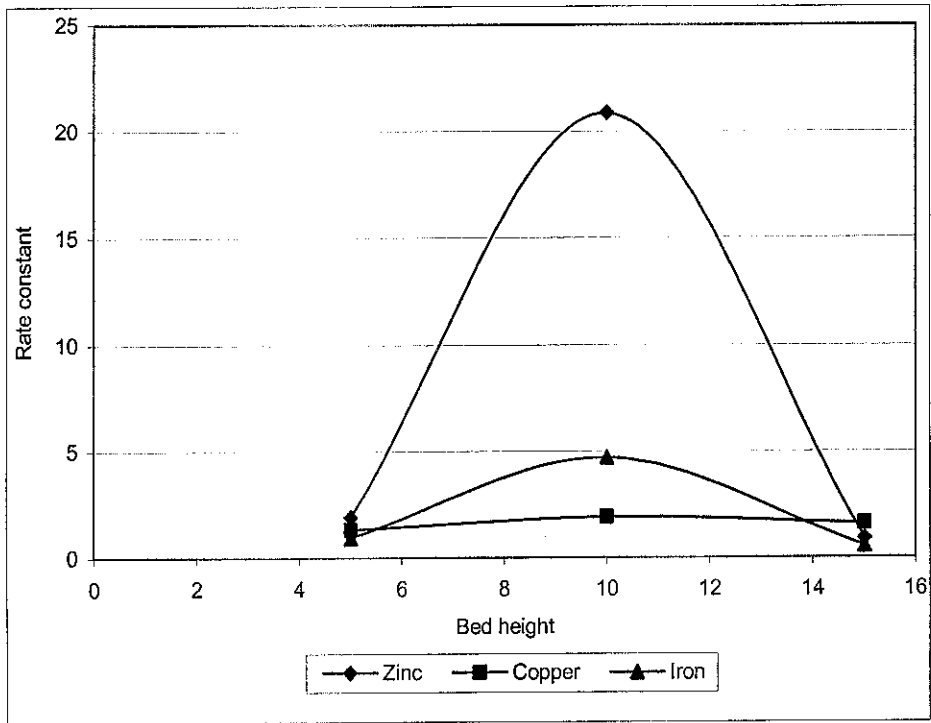


Figure 4.9(a) : Relationship between the rate constant (k_{YN}) with bed height

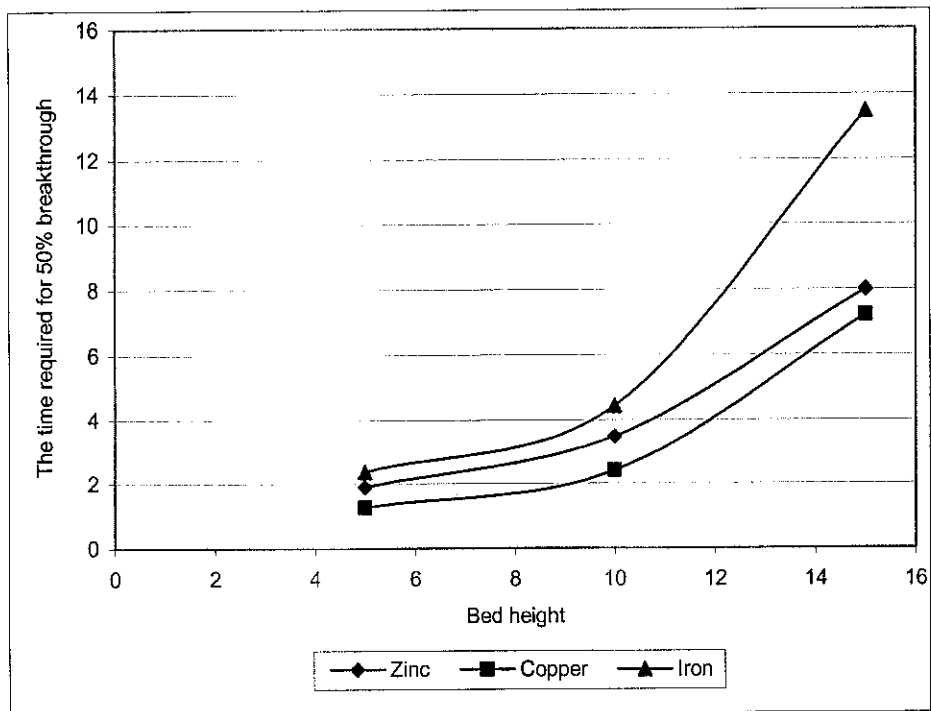


Figure 4.9(b) : Relationship between the time required for 50% breakthrough (τ) with bed height

The values of k_{YN} and τ are listed in Table 4.3. From Table 4.3, the rate constant k_{YN} increased and the 50% breakthrough time τ also increased with decreasing flow rate. With the bed volume increasing, the values of τ increased while the values of k_{YN} fluctuated. The data in Table 4.3 also indicated that values τ from the calculation were significantly different compared to experimental results.

Table 4.3 : Yoon–Nelson parameters at different conditions using non-linear regression analysis

Yoon-Nelson Model

	C_0 (mg/L)	v (ml/min)	Z (cm)	K_{YN}	τ	R^2
Zinc	9.40	24	5	1.929	1.911	0.988
	9.00	13	10	20.890	3.477	0.852
	9.00	6	15	0.910	7.995	0.886
Copper	16.10	24	5	1.328	1.286	0.800
	16.10	13	10	1.909	2.419	0.942
	16.10	6	15	1.602	7.213	0.991
Iron	9.90	24	5	0.953	2.372	0.866
	9.90	13	10	4.718	4.439	0.856
	9.90	6	15	0.547	13.461	0.977

CHAPTER 5 : CONCLUSION AND RECOMMENDATION

From the analysis that have been conducted for Zinc, Copper and Iron, the heavy metal in the adsorption column reach the breakthrough with different adsorption rate.

The Microwaved Incenerated Rice Husk Ash (MIRHA) has a capable of removing over **100%** of Zinc, Copper and Iron from aqueous solution and MIRHA is an effective adsorbent for Zn, Cu and Fe. The rate of adsorption process also different for every each of the heavy metal.

The initial region of breakthrough curve was defined by Adams-Bohart model at all experimental condition studied while the full description of breakthrough could be accomplished by Thomas models.

REFERENCES

1. Aksu and Gonen, (2004). Biosorption of phenol by immobilized activated sludge in a continuous packed bed: Prediction of breakthrough curves, *Process Biochem.* 39, pp. 599–613.
2. Benito Y. and Ruiz, M.L., (2002). Reverse osmosis applied to metal finishing wastewater. *Desalination*, vol. 142, no. 3, p. 229-234.
3. G. McKay, J.F. Porter and G.R. Prasad, The removal of dye colour from aqueous solutions by adsorption on low-cost materials, *Water Air Soil Poll.* 114 (1999), pp. 423–438.
4. H.A. Elliott and C.P. Huang, (1981) Adsorption characteristics of some Cu(II) complexes on aluminosilicates, *Water Res.* 15, pp. 849–854.
5. J.W. Patterson, (1977). *Wastewater Treatment*, Science Publishers, New York.
6. Kortenkamp, A. et al., (1996). *Archives of Biochemistry and Biophysics*, vol. 329, no. 2, p. 199-208.
7. Kumar and Sivanesan, (2006). Equilibrium data, isotherm parameters and process design for partial and complete isotherm of methylene blue onto activated carbon, *J. Hazard. Mater.* 131 (2006), pp. 217–228.
8. Lester J.N. (1987). *Heavy Metals in Wastewater and Sludge Treatment Processes. Volume 1, Sources Analysis, and Legislation.* CRC Press, Inc., Boca Raton, Florida. p 157-159.
9. M. H. Isa et al., (2004). Fe removal by adsorption using Ash from oil farm factory. *Universiti Sains Malaysia, Engineering Campus, Penang, Malaysia.* p 2-4.

10. Q. Feng, Q. Lin, F. Gong, S. Sugita and M. Shoya, (2004) Adsorption of lead and mercury by rice husk ash, *J. Colloid Interf. Sci.* 278, pp. 1–8.
11. R.P. Han, J.H. Zhang, W.H. Zou, H.J. Xiao, J. Shi and H.M. Liu, Biosorption of copper(II) and lead(II) from aqueous solution by chaff in a fixed-bed column, *J. Hazard. Mater.* 133 (2006), pp. 262–268.
12. Rengaraj, S.; Yeon, K.H. and Moon, (2001). S.H. Removal of chromium from water and wastewater by ion exchange resins. *Journal of Hazardous Materials*, vol. 87, no. 1-3, p. 273-287.
13. Reynolds, T.D., Richards, P.A., (1995). *Unit Operations and Processes in Environmental Engineering*. PWS Publishing Company, Boston, Massachusetts.
14. S.P. Mishra, D. Tiwari and R.S. Dubey, (1997). The uptake behavior of rice (jaya) husk in the removal of Zn(II) ions a radiotracer study, *Appl. Radiat. Isot.* 48, pp. 877–882.
15. Shamsul Rahman M. Kutty, (2001). *Removal of Heavy Metals Using Rice Husk Ash*.
16. T.G. Chuah et al., (2004). Rice husk as a potentially low-cost biosorbent for heavy metal and dye removal. *Desalination* 175, p. 305-316.
17. Vijayaraghavan et al., (2004). Removal of nickel(II) ions from aqueous solution using crab shell particles in a packed bed up-flow column, *J. Hazard. Mater.* 113, pp. 223–230.
18. Weber, W.J, (1972). *Physiochemical Process for Water Quality Control*. Wiley-Interscience, Inc., Canada. p 199-211.

19. Yan and Viraraghavan, 2001 G.Y. Yan and T. Viraraghavan, Heavy metal removal in a biosorption column by immobilized *M. rouxii* biomass, *Bioresour. Technol.* 78 (2001), pp. 243–249.
20. Yurlova, L., Kryvoruchko, A. and Kornilovich, B, (2002). Removal of Ni (II) ions from wastewater by micellar-enhanced ultrafiltration. *Desalination*, vol. 144, no. 255-260.

APPENDICES

LIST OF APPENDIX

Appendix A-1 : Apparatus setup adsorption column.....	32
Appendix A-2 : Example of the breakthrough curve.....	33
Appendix A-3: Breakthrough curves for various adsorption bed heights.....	34
Appendix B-1 : Flowrate calibration for determine the pump speed.....	35
Appendix C-1 : Adsorption datasheet for Zinc ($C_0 = 9.4$ mg/L).....	36
Appendix C-2 : Adsorption datasheet for Copper ($C_0 = 16.1$ mg/L).....	37
Appendix C-3 : Adsorption datasheet for Iron ($C_0 = 9.9$ mg/L).....	38

Appendix A-1

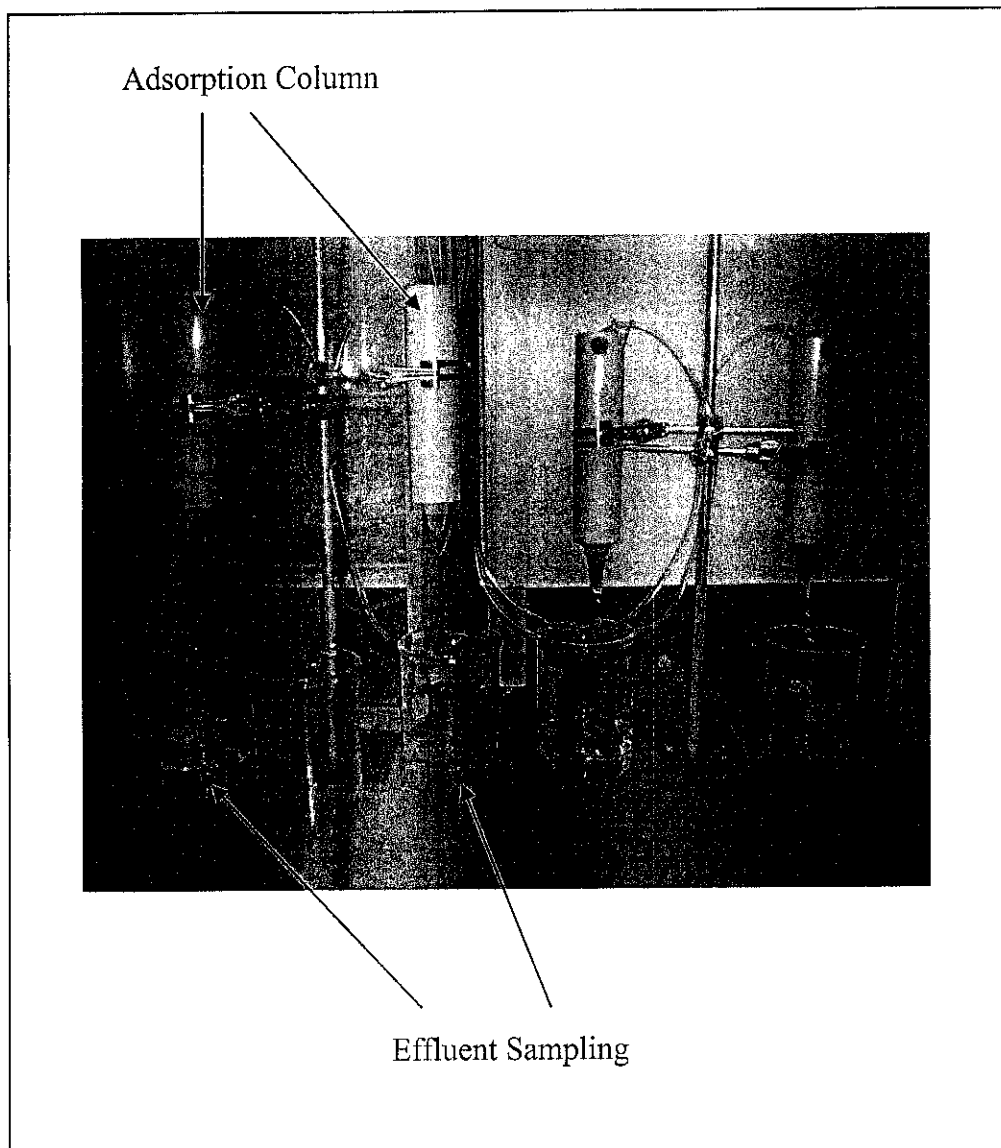


Figure : Apparatus setup adsorption column

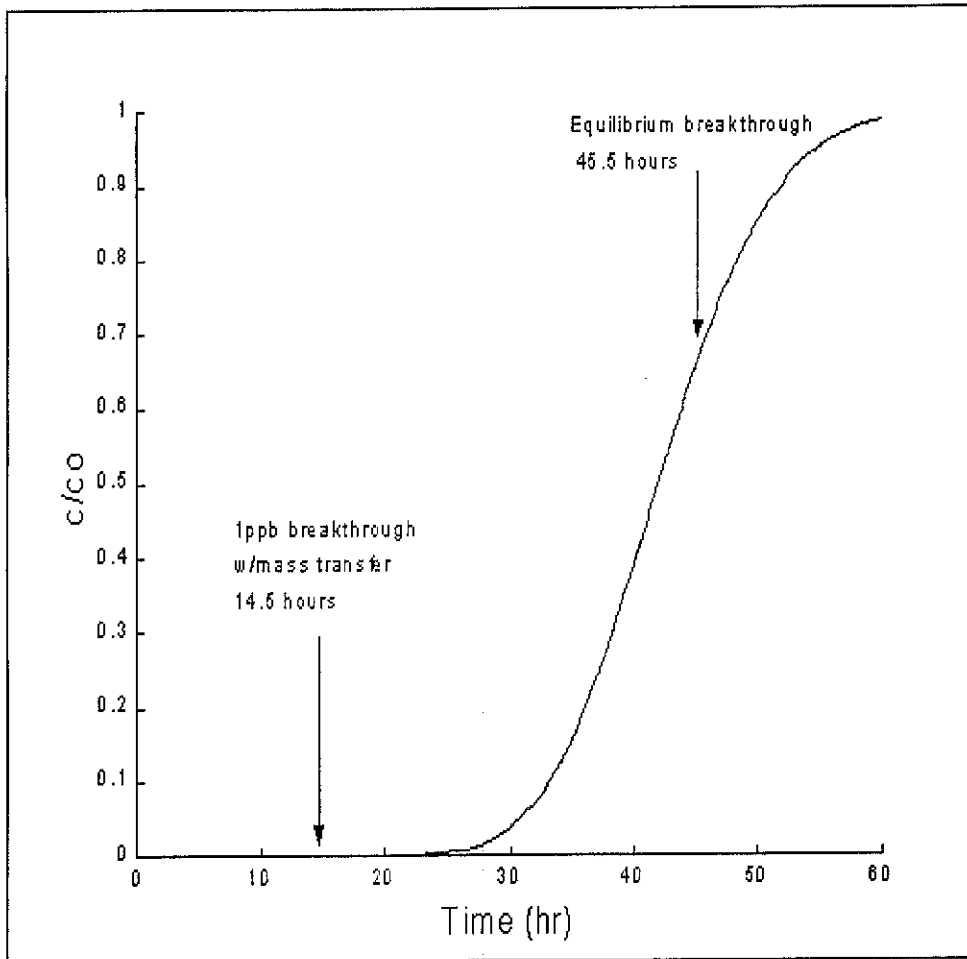


Figure 2.4 : Example of the breakthrough curve

Appendix A-3

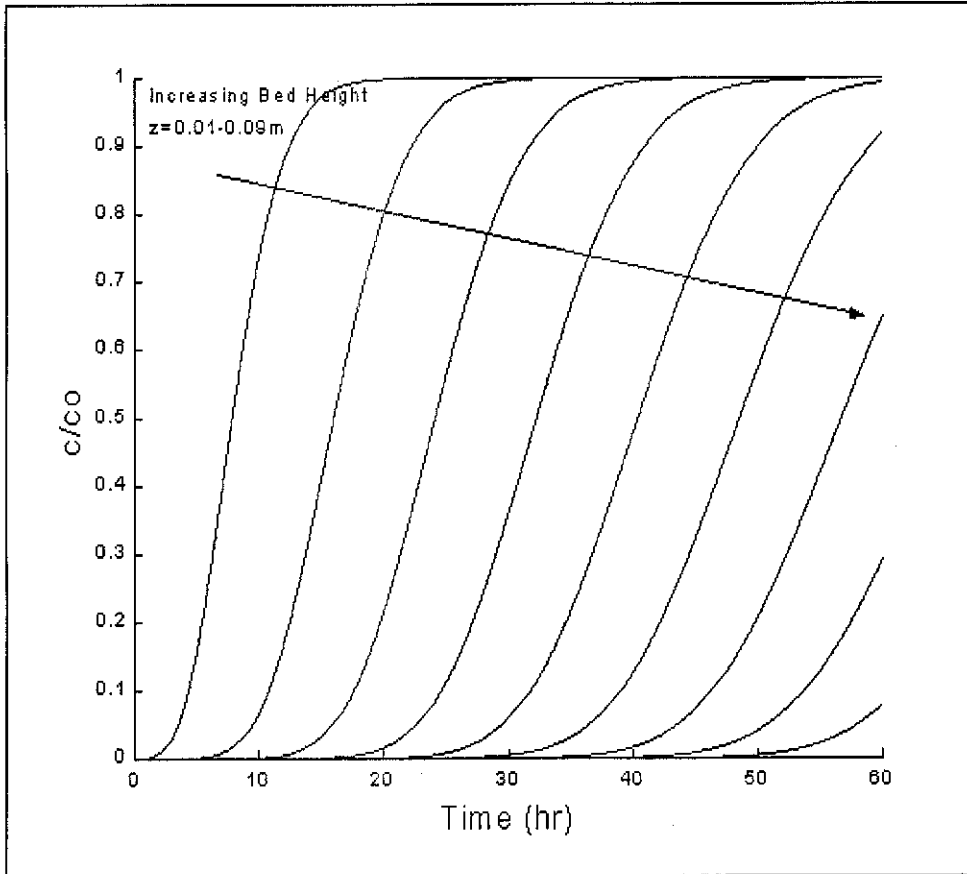


Figure 2.4.1 : Breakthrough curves for various adsorption bed heights

Appendix B-1

No	Effluent Flowrate			Pump Speed (rev/min)
	ml / day	ml / hour	ml / minute	
1	500	20.83	0.35	0.1
2	800	33.33	0.56	0.2
3	1000	41.67	0.69	0.3
4	2000	83.33	1.39	0.6
5	5000	208.33	3.47	1.4
6	10000	416.67	6.94	2.8
7	15000	625.00	10.42	4.2
8	20000	833.33	13.89	5.6

Table 4.1 : Flowrate calibration for determine the pump speed

Appendix C-1

Hour	Bed Height 5 cm		Bed Height 10 cm		Bed Height 15 cm	
	Concentration (C)	C / Co	Concentration (C)	C / Co	Concentration (C)	C / Co
1	0.08	0.01	0.07	0.01	0.02	0.00
2	1.19	0.13	0.06	0.01	0.06	0.01
3	2.38	0.25	0.47	0.05	0.06	0.01
4	3.40	0.36	1.41	0.16	0.06	0.01
5	8.50	0.90	5.00	0.56	0.07	0.01
6	9.45	1.01	7.00	0.78	0.04	0.00
7	9.50	1.01	8.00	0.89	0.06	0.01
8			8.60	0.96	0.04	0.00
9			8.90	0.99	0.18	0.02
10			8.97	1.00	0.60	0.07
11			8.96	1.00	0.91	0.10
12					1.52	0.17
13					2.50	0.28
14					3.50	0.39
15					5.20	0.58
16					6.10	0.68
17					6.40	0.71
18					6.70	0.74
19					7.00	0.78
20					7.20	0.80
21					7.50	0.83
22					7.90	0.88
23					8.20	0.91
24					8.50	0.94
25					8.70	0.97
26					8.80	0.98
27					9.00	1.00
28						
29						
30						

Table 4.2.1 : Adsorption datasheet for Zinc (Co = 9.4 mg/L)

Appendix C-2

Hour	Bed Height 5 cm		Bed Height 10 cm		Bed Height 15 cm	
	Concentration (C)	C / Co	Concentration (C)	C / Co	Concentration (C)	C / Co
1	0.05	0.00	0.01	0.00	0.03	0.00
2	2.47	0.15	0.03	0.00	0.03	0.00
3	11.70	0.73	0.98	0.06	0.02	0.00
4	16.10	1.00	3.18	0.20	0.03	0.00
5	16.10	1.00	10.20	0.63	0.24	0.02
6			13.60	0.84	0.80	0.05
7			15.00	0.93	1.20	0.08
8			16.10	1.00	2.10	0.13
9			16.10	1.00	5.40	0.34
10					9.20	0.58
11					10.90	0.69
12					11.70	0.74
13					12.40	0.78
14					12.70	0.80
15					13.20	0.83
16					13.30	0.84
17					13.80	0.87
18					14.40	0.91
19					14.50	0.91
20					14.90	0.94
21					15.20	0.96
22					15.30	0.96
23					15.50	0.97
24					15.60	0.98
25					15.90	1.00
26					15.80	0.99
27						
28						
29						
30						

Table 4.2.2 : Adsorption datasheet for Copper (Co = 16.1 mg/L)

Appendix C-3

Hour	Bed Height 5 cm		Bed Height 10 cm		Bed Height 15 cm	
	Concentration (C)	C / Co	Concentration (C)	C / Co	Concentration (C)	C / Co
1	0.01	0.00	0.01	0.00	0.02	0.00
2	0.02	0.00	0.00	0.00	0.02	0.00
3	1.20	0.12	0.00	0.00	0.02	0.00
4	1.93	0.19	0.39	0.04	0.02	0.00
5	4.20	0.42	1.58	0.16	0.60	0.06
6	7.50	0.76	2.90	0.29	0.87	0.09
7	8.60	0.87	3.90	0.39	0.94	0.09
8	9.80	0.99	4.70	0.47	1.14	0.12
9	9.90	1.00	5.60	0.57	1.27	0.13
10			7.10	0.72	1.34	0.14
11			8.10	0.82	1.47	0.15
12			9.70	0.98	1.72	0.17
13			9.80	0.99	1.78	0.18
14			9.90	1.00	1.92	0.19
15					2.15	0.22
16					2.47	0.25
17					2.74	0.28
18					3.10	0.31
19					3.84	0.39
20					4.70	0.47
21					4.80	0.48
22					5.00	0.51
23					5.30	0.54
24					5.60	0.57
25					5.80	0.59
26					6.20	0.63
27					6.20	0.63
28					6.30	0.64
29					6.50	0.66
30					6.60	0.67
31					6.80	0.69
32					7.10	0.72
33					7.20	0.73
34					7.30	0.74
35					7.50	0.76
36					7.90	0.80
37					8.10	0.82
38					8.40	0.85
39					8.70	0.88
40					8.80	0.89
41					9.00	0.91
42					9.30	0.94
43					9.60	0.97
44					9.80	0.99
45					9.90	1.00

Table 4.2.2 : Adsorption datasheet for Iron ($C_o = 9.9 \text{ mg/L}$)